Alfvénic turbulence in slow solar wind streams: an overview

Raffaella D'Amicis

INAF - IAPS, Rome, Italy

Collaborators:

R. Bruno, M. Velli, D. Perrone, O. Panasenco, L. Matteini, D. Telloni, M. F. Marcucci, L. Woodham, R. De Marco, V. Jagarlamudi, I. Coco, C. Owen, P. Louarn, S. Livi, T. Horbury, K. Alielden, N. André, V. Angelini, V. Evans, A. Fedorov, V. Génot, B. Lavraud, S. T. Lepri,, D. Müller, H. O'Brien, O. Pezzi, J. M. Raines, A. P. Rouillard, L. Sorriso-Valvo, A. Tenerani, D. Verscharen, L. Zhao, and I. Zouganelis

ISSI Team 'Turbulence at the Edge of the Solar Corona: Constraining Available Theories Using the Latest Parker Solar Probe Measurements'

Traditional classification of the solar wind according to the flow speed

- **Different density, proton and electron temperature** (Lopez & Freeman, 1986; Schwenn, 2006)
- **Electron strahl in fast wind** (papers by Pilipp et al.)
- **Anticorrelation between freeze-in temperature and speed** (Geiss et al., 1995; Kasper et al., 2012)
- **FIP effect in slow wind** (Geiss et al., 1995; Zurbuchen et al., 1999; von Steiger et al., 2000)
- **Different solar sources** (Abbo et al., 2016, and references therein)

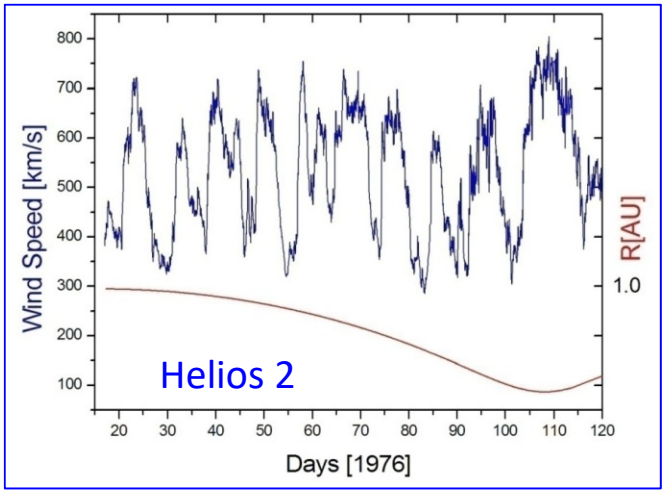

Traditionally categorized in fast (v > 600 km/s) and slow (v < 500 km/s) solar wind

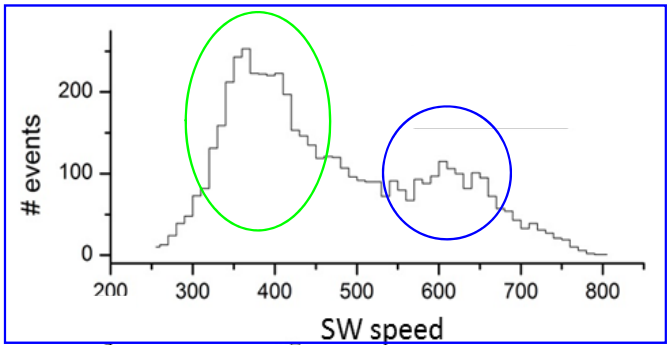

Alfvénicity in the solar wind

Large amplitude Alfvénic fluctuations are very common features in the solar wind

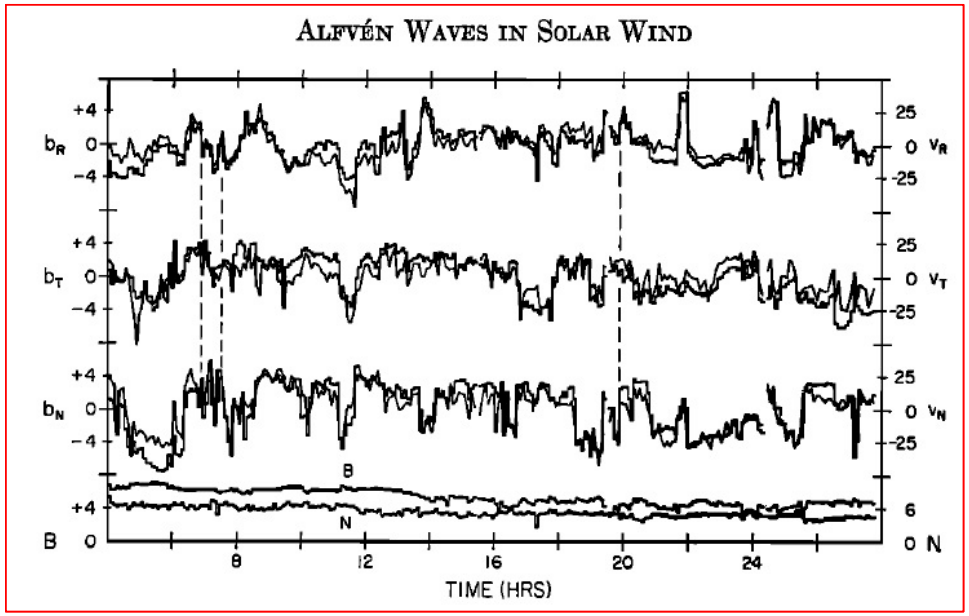

(Belcher & Solodyna, 1975)

Fast wind more Alfvénic than slow wind

- Larger amplitude fluctuations in fast wind
- Anisotropy and beams in fast wind VDF
- Ion drift in fast wind
- Different spectral features

Constant B magnitude

Tip of magnetic field vector constrained to move on a sphere

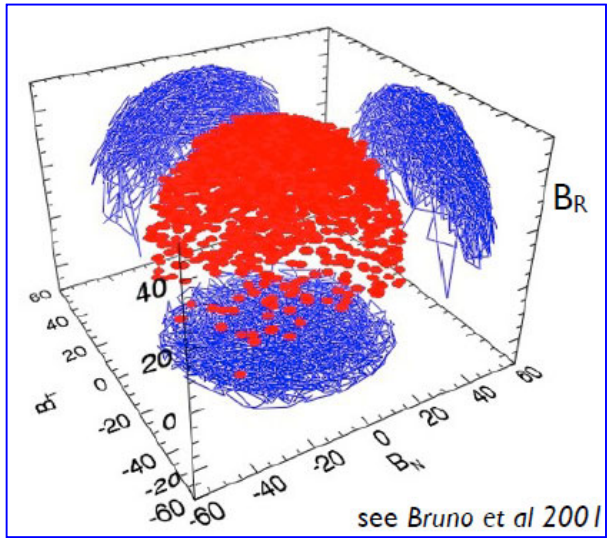

Evolution of the Alfvénic content

$$\delta V = sign[-k \cdot B_0] \frac{\delta B}{\sqrt{4\pi\rho}}$$

FAST WIND

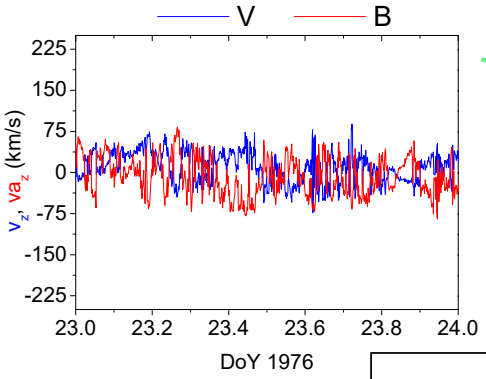

0.9 AU

SLOW WIND

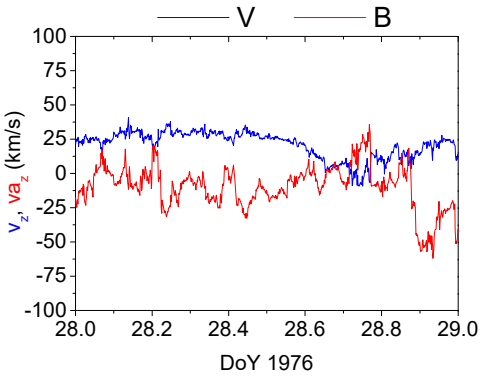

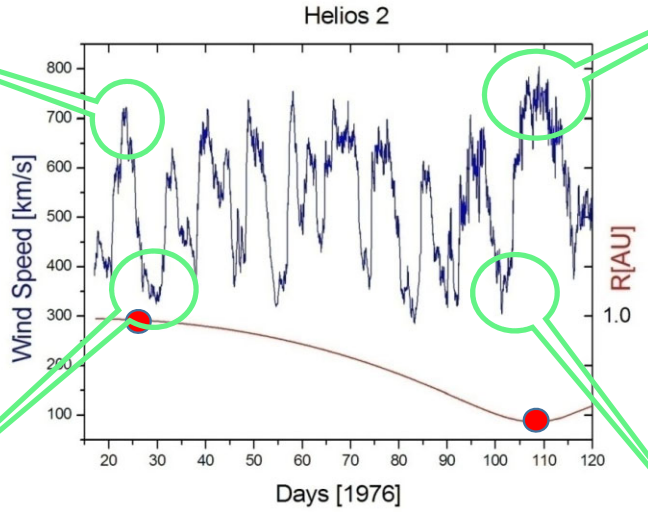

FAST WIND

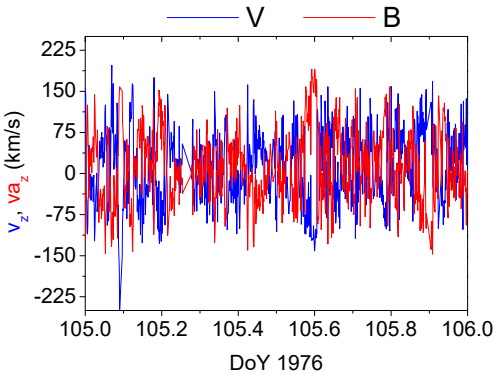

0.3 AU

SLOW WIND

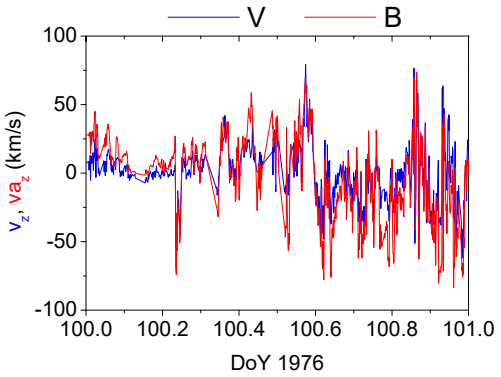

Effects of the radial evolution:
decrease of fluctuation amplitude and
Alfvénicity is lost in the slow wind

Peculiar slow wind – first observation

The first observation of a peculiar slow solar wind occurred during the ascending phase of solar cycle 21 around 0.29 AU (Helios perihelion).

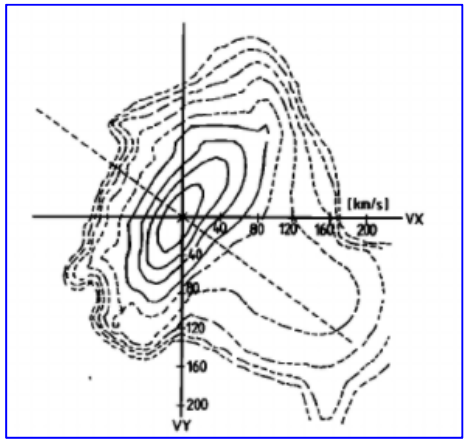

Large proton temperature anisotropies

Pronounced differential speeds between proton and alpha particles bulk flows

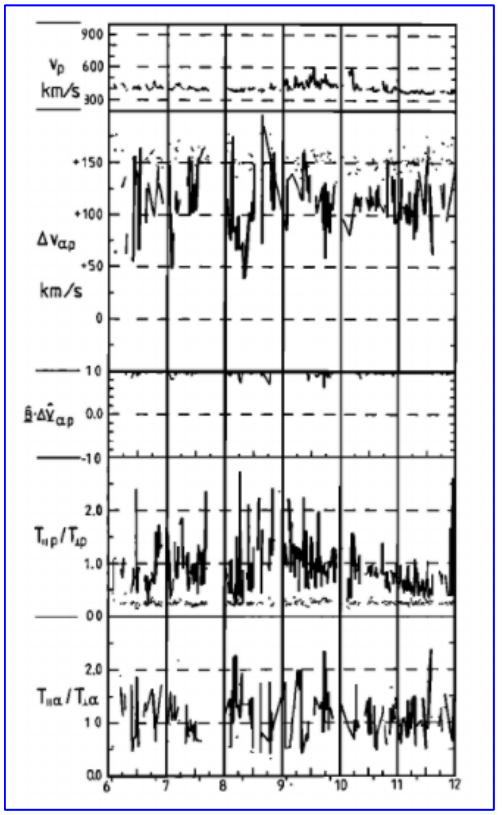

(*Marsch et al 1981*)

All these features, along with the typical signature of Alfvénic fluctuations, were very similar to what is observed in the fast wind.

Alfvénic slow wind at 1AU - statistical study

Normalized cross-helicity

$$\sigma_C = \frac{e^+ - e^-}{e^+ + e^-}$$

Example of Alfvénic slow wind

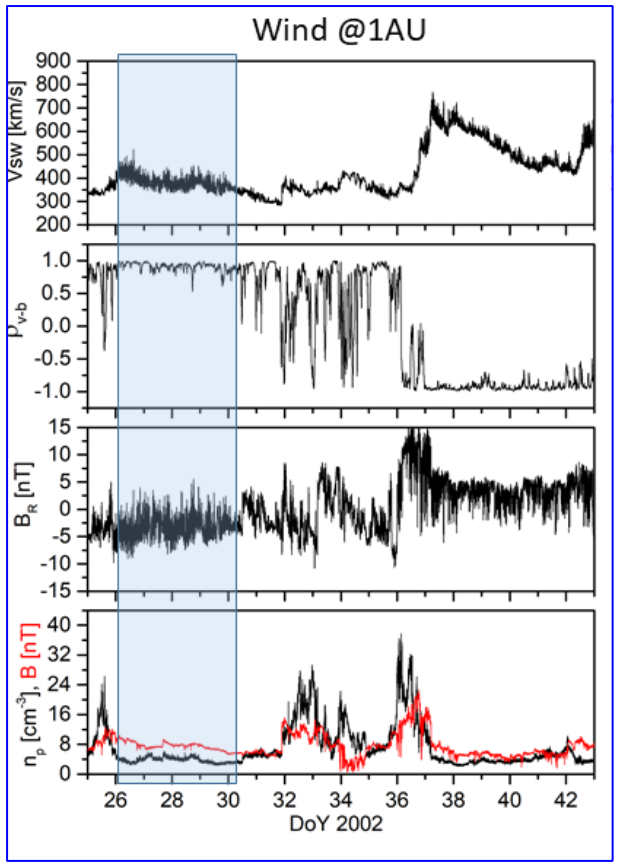

(adapted from D'Amicis et al, JGR, 2021)

(Adapted from D'Amicis & Bruno, ApJ, 2015)

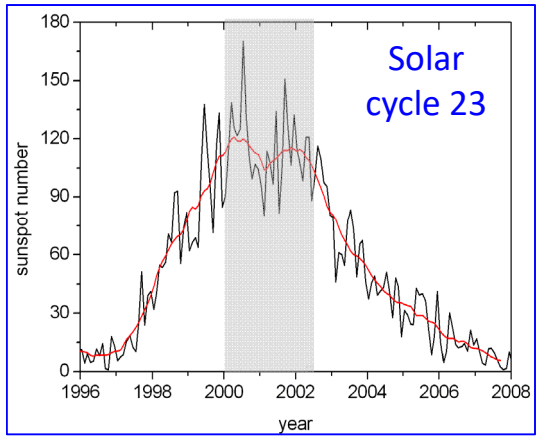

Maximum of solar cycle

Alfvénic slow wind

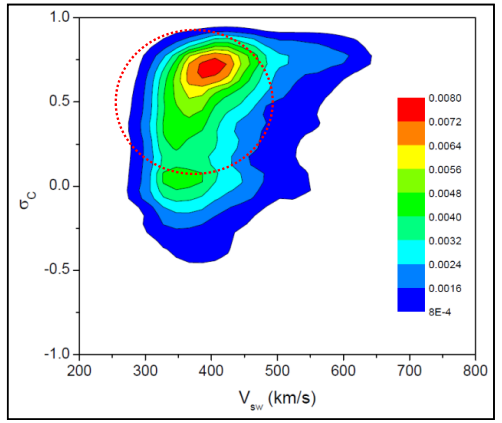

Not an isolated case, rather a statistical result (*D'Amicis et al, JASTP, 2011*) found with measurements at 1 AU where a degradation of the v-b correlation is expected.

Alfvénicity in solar cycle 23 and 24

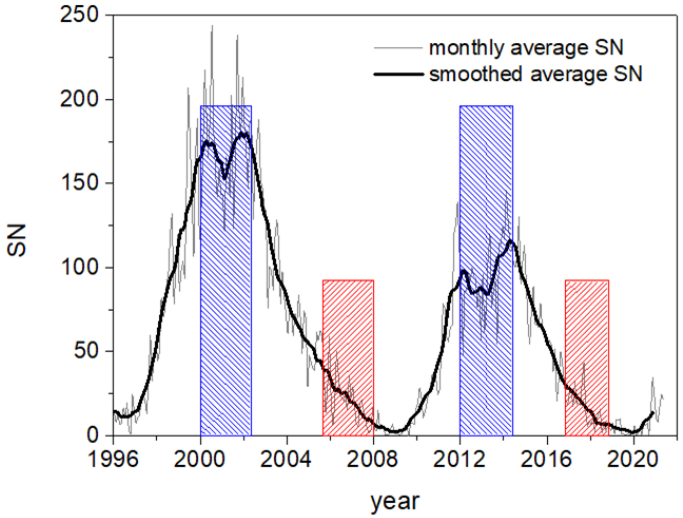

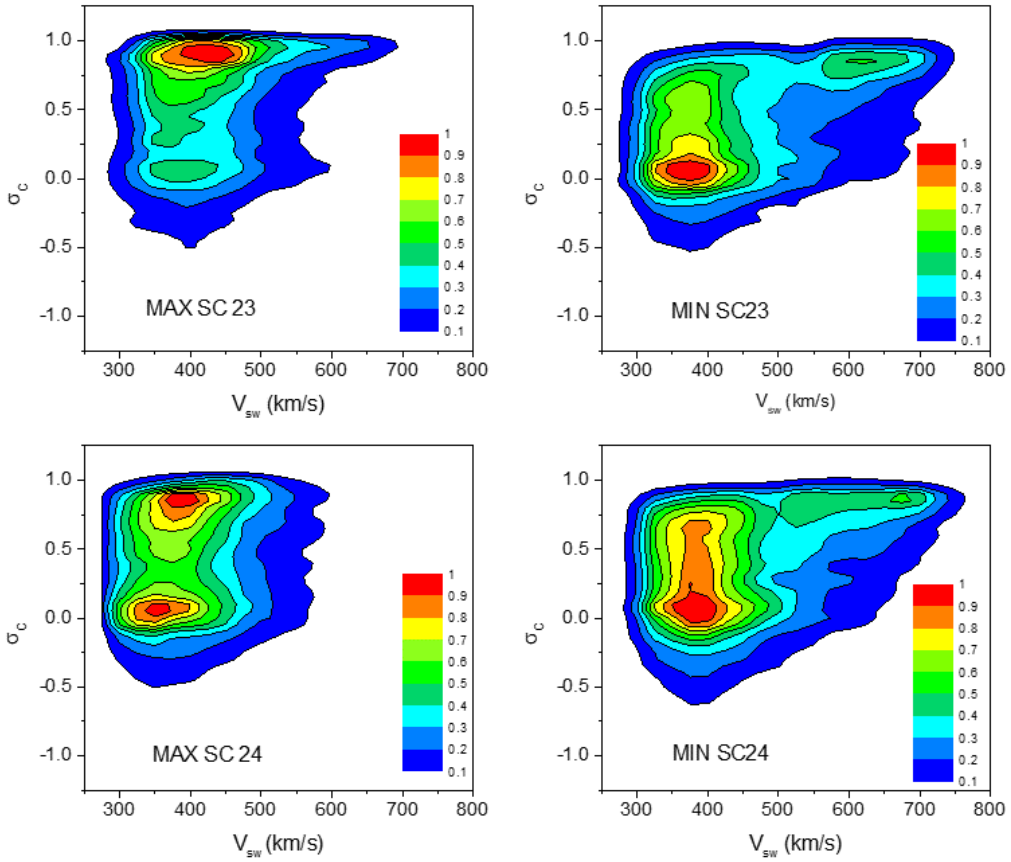

D'Amicis et al, A&A 654, A111 (2021)

Similarities with the fast wind

- high Alfvénic content,
- large v and b fluctuations
- low compressibility,
- low turbulence age,
- low β,
- similar spectral properties,
- low O^{7+}/O^{6+} ratio and similar solar source

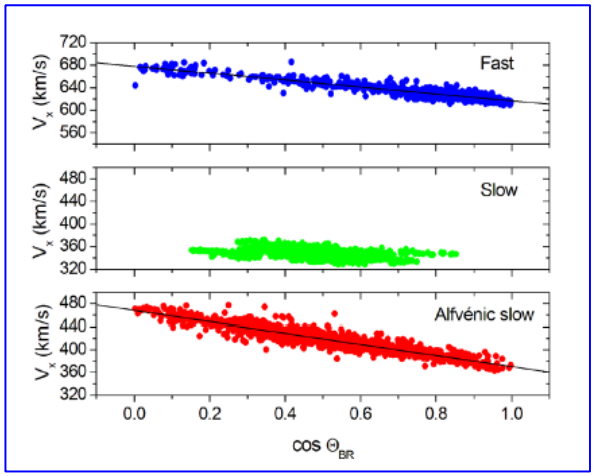

θ_{BR} – V_{SW} relationship (1AU)

$$V_p \sim V_0 + v_{ph}[1 - \cos(\Theta_{BR})],$$

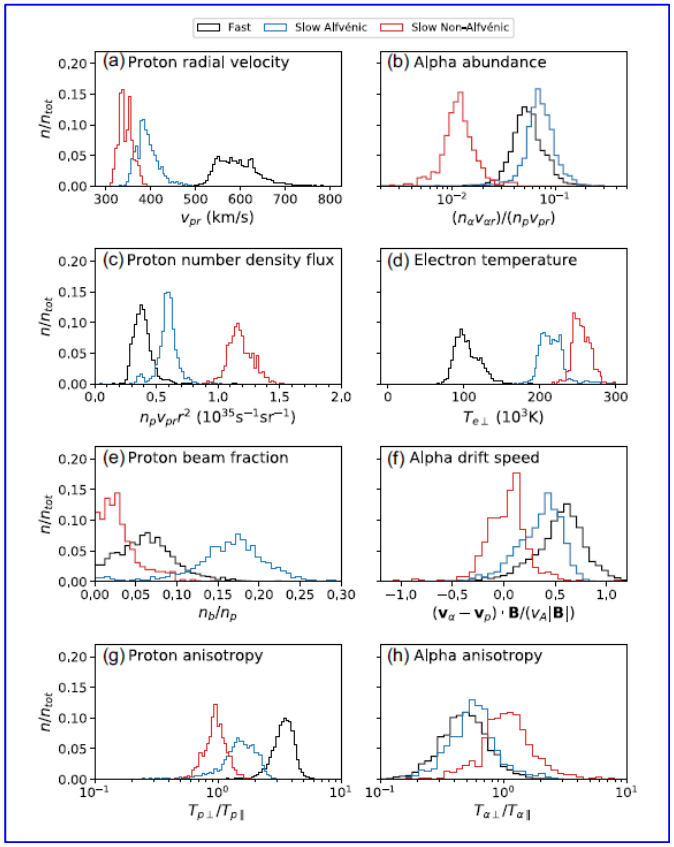

(*D'Amicis et al MNRAS 2019, Sol. Phys, 2020; Stansby et al MNRAS 2019; Perrone et al. A&A 2020, D'Amicis et al JGR 2021*)

- alpha particle abundance, alpha-to-proton temperature ratio, and alpha particle drift speed (0.3 AU)

anticorrelation $\beta_{||}$ - anisotropy (1 AU)

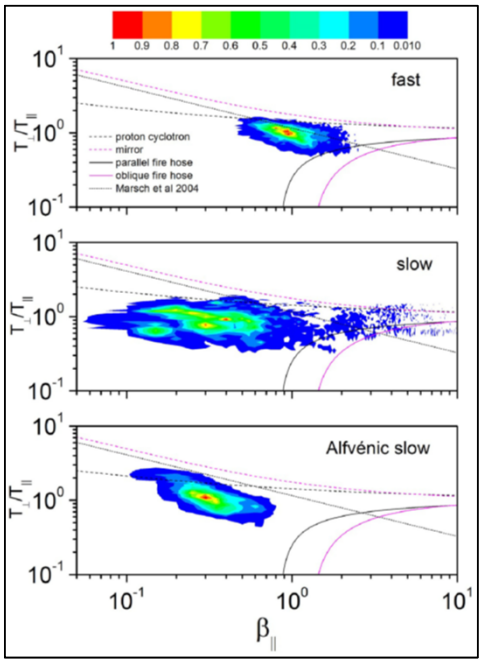

Solar sources

Lower O and C ratios characterize the Alfvénic time intervals thus suggesting a similar solar origin of the two plasma flows, i.e. open field regions of anomalous areal expansion of magnetic flux tubes → *boundaries of polar coronal holes an/or low-latitude small coronal holes*

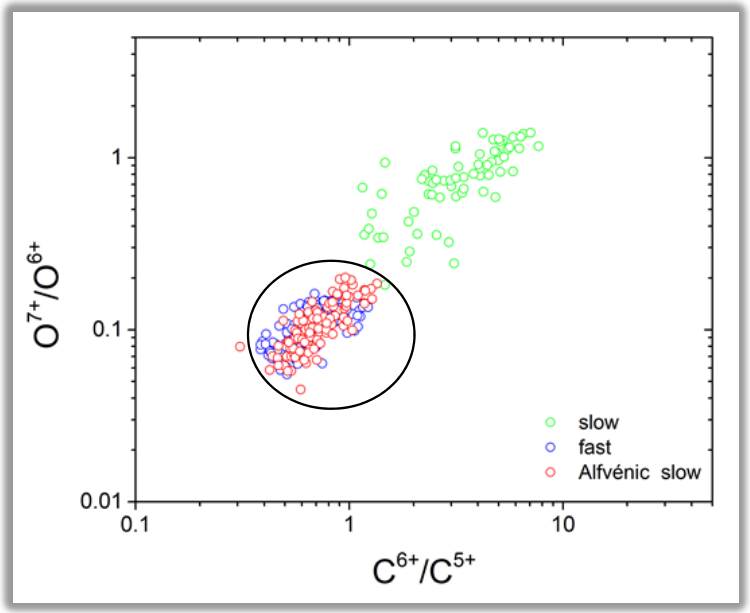

(D'Amicis et al, JGR, 2021a)

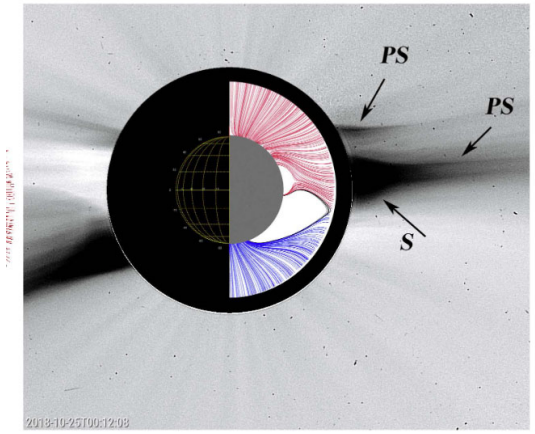

EUV synoptic map

A composite view of two images, one by the LASCO/C2 camera taken on 2018 October 25 00:12 UT and one of the PFSS model (Panasenco et al, ApJS, 2020).

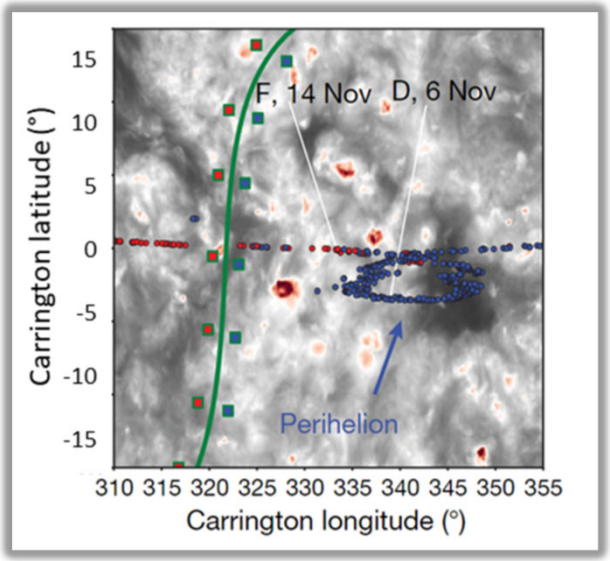

(Bale et al, Nature, 2019)

PSP Encounter1

Low latitude small coronal hole in the presence of a pseudostreamer configuration

Pseudostreamers and strong divergence

(adapted from D'Amicis et al, A&A, 2021c)

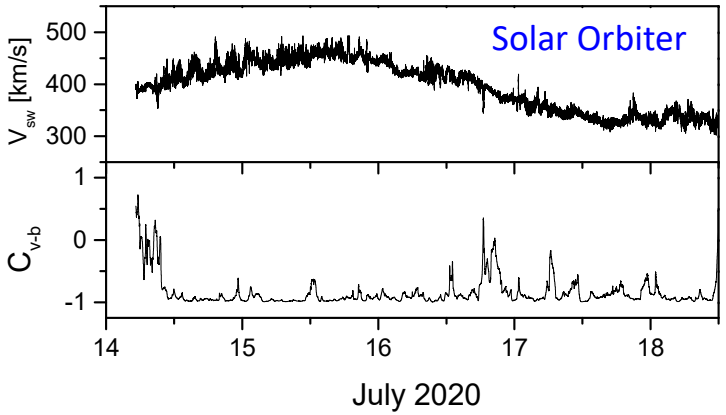

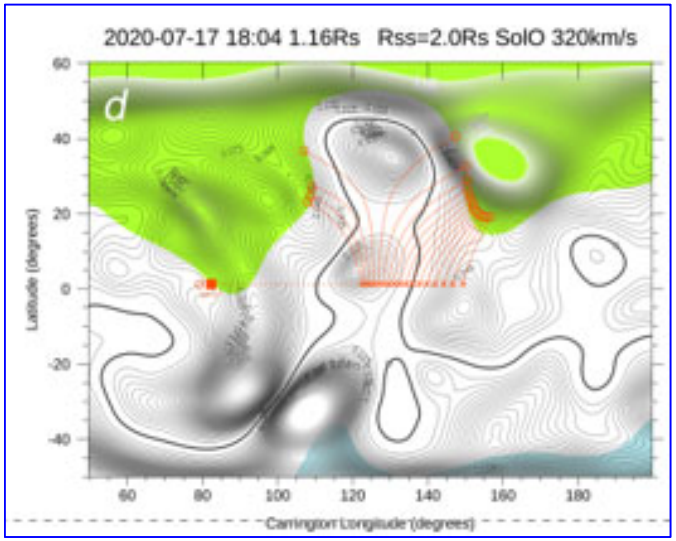

Multipolar regions separating coronal holes with the same polarity

- The topology of pseudostreamers allows the formation and development of twin filament channels that create conditions for a strong divergence of the field and that are also related to a strong non-monotonic expansion of the open magnetic field lines (Panasenco & Velli, 2013; Panasenco et al 2019).
- This would slow down the fast solar wind, setting the conditions for the development of the Alfvénic slow solar wind → important for the general problem of solar wind acceleration.

https://www.sidc.be/silso/kalmanml

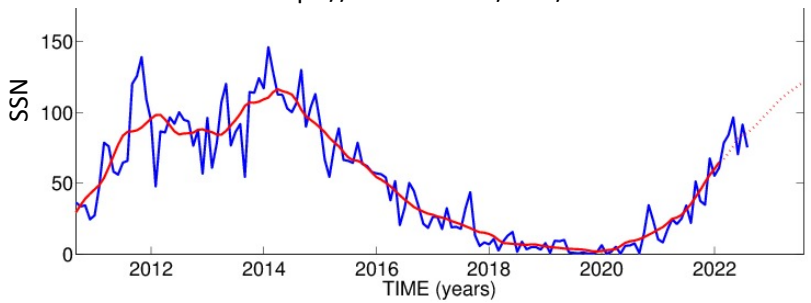

➢ Very timely since we are approaching the maximum of solar activity characterized by a statistical predominance of the Alfvénic slow wind (e.g. D'Amicis et al 2011, 2021b).

Comparing fast and Alfvénic slow PSD

Wind data @ 1 AU

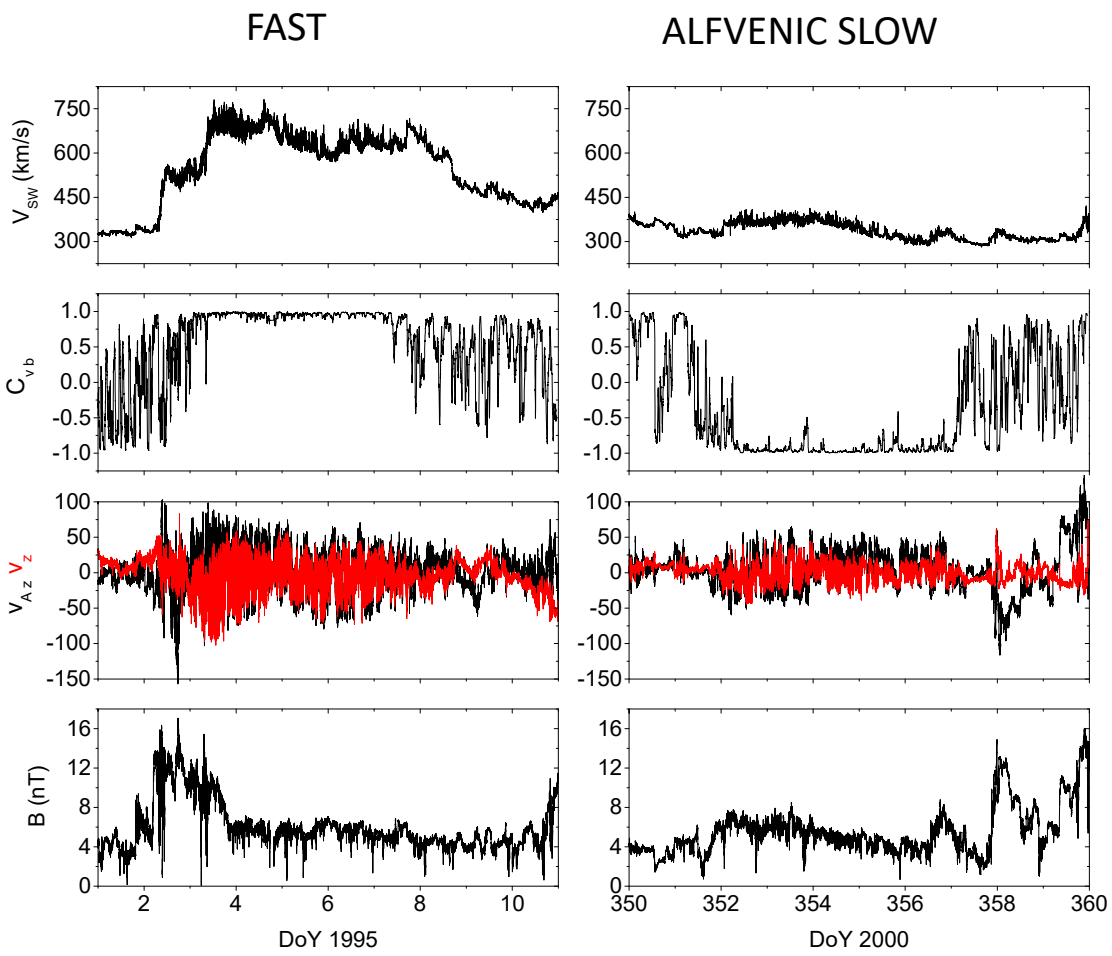

(D'Amicis et al Sol. Phys. 2020)

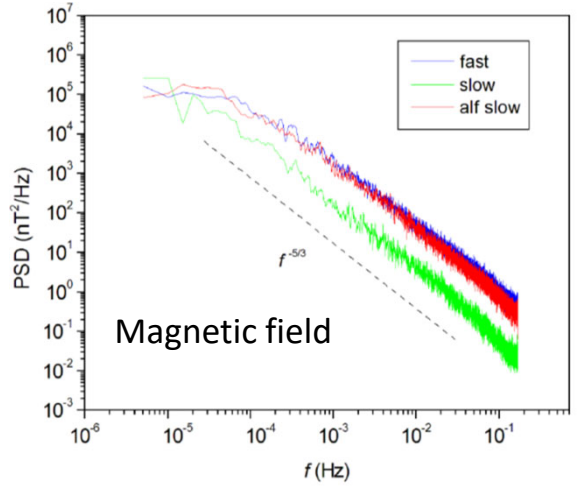

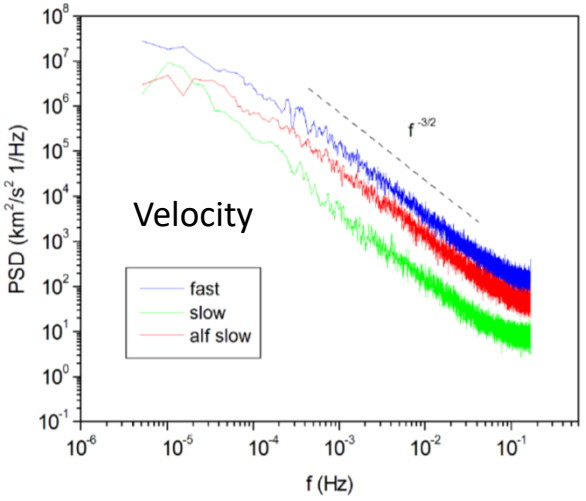

Fast
Slow
Alfvénic slow

Normalized spectra

$$\delta B(f) = \sqrt{2 f P_B(f)}$$

Fourier spectrum

@ 1 AU

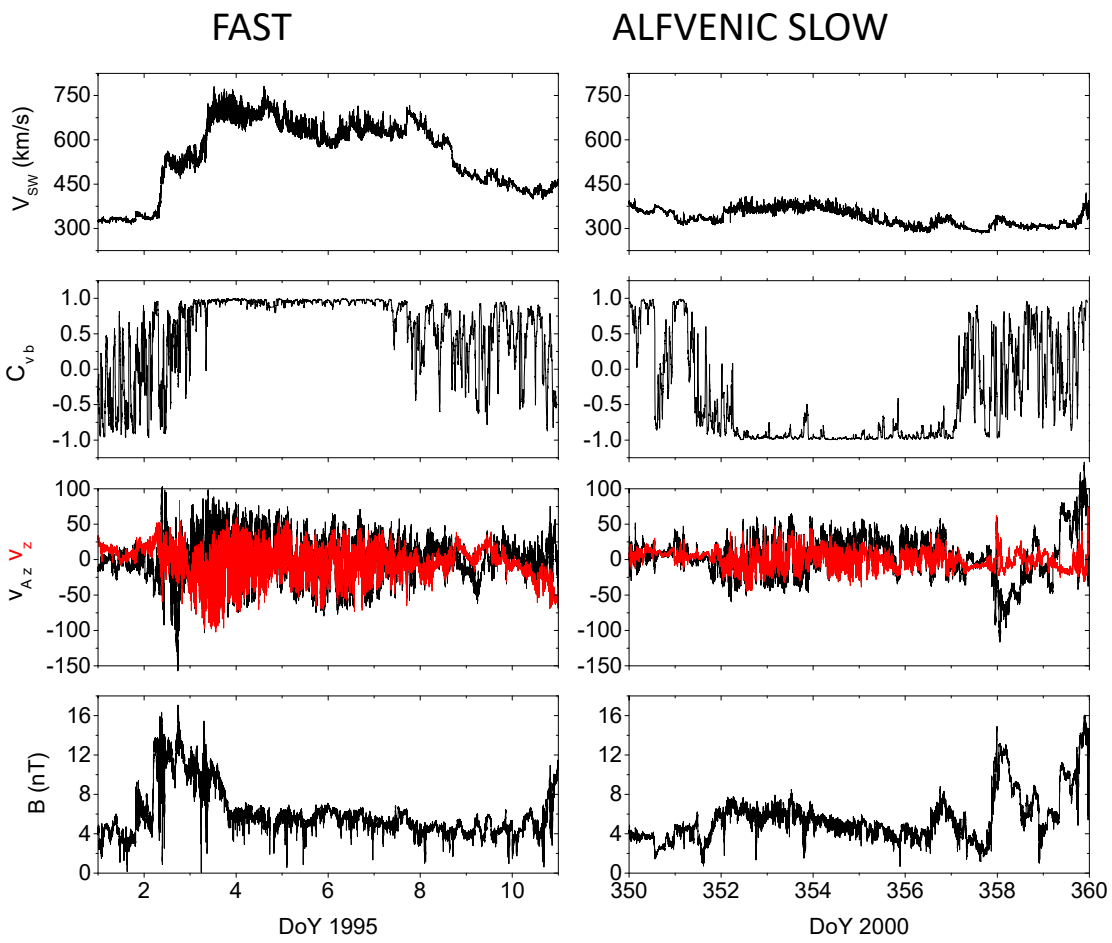

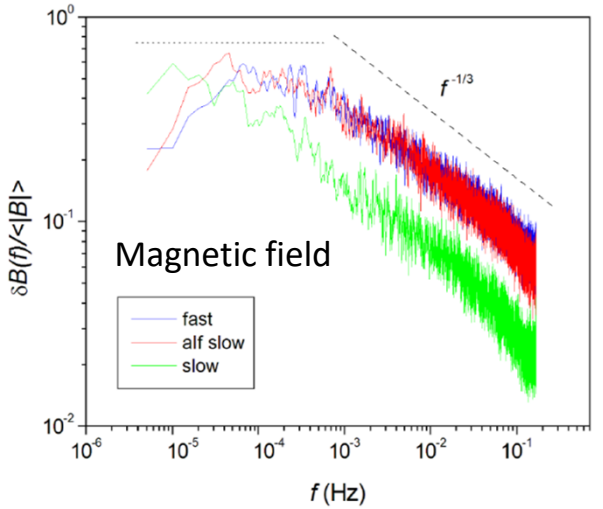

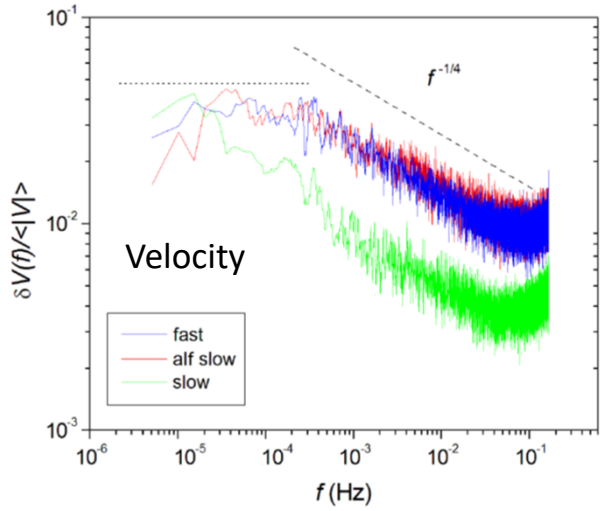

Fast
Slow
Alfvénic slow

(D'Amicis et al Sol. Phys. 2020)

Alfvénic turbulence in fast and Alfvénic slow streams

V-b correlation coefficient

Ratio of the amplitude of magnetic field fluctuations and the amplitude of the magnitude

Relative amplitude of number density compared to turbulent Mach number squared

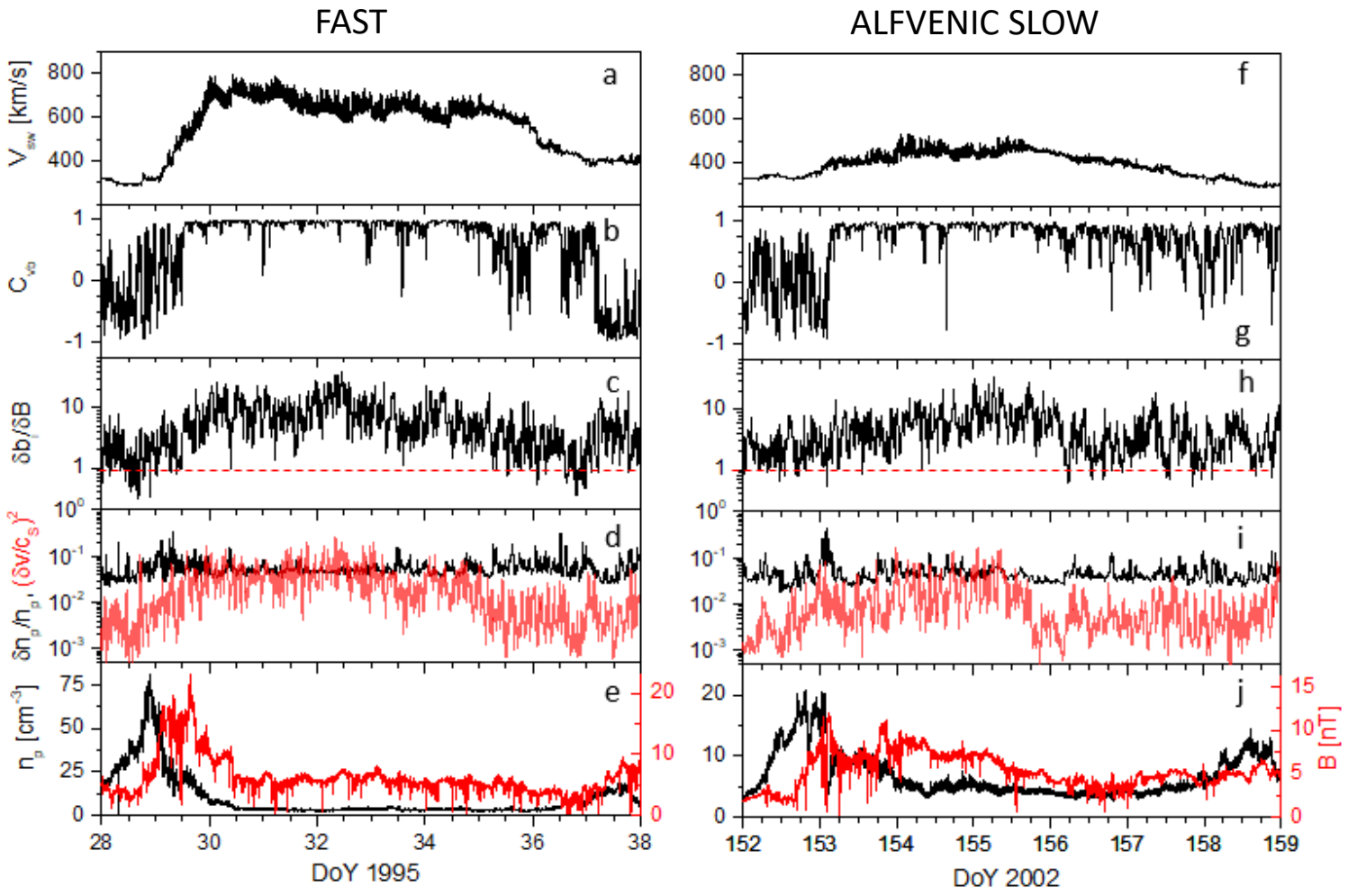

(D'Amicis et al. Universe, 2022)

Spectral analysis – normalized power spectra

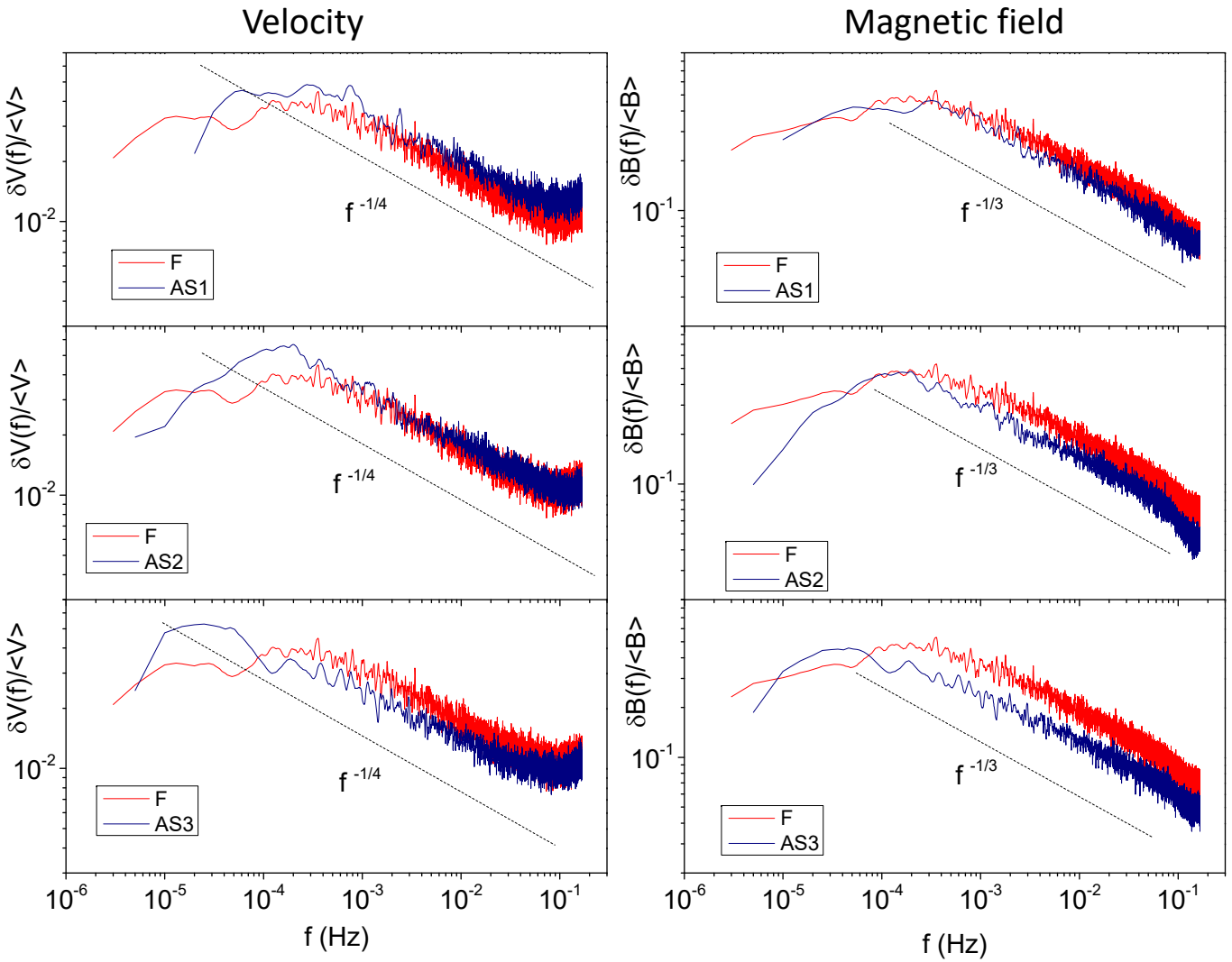

Comparison between fast (F, red) and Alfvénic slow streams (AS1, AS2, AS3, blue)

Comparable power of the fluctuations

Velocity spectra scaling as $f^{-3/2}$
Magnetic field spectra scaling as $f^{-5/3}$

$$\delta B(f) = \sqrt{2 f P_B(f)}$$

(D'Amicis et al., Universe, 2022)

Spectral behaviour of σ_C and σ_R

$$\sigma_C(f) = \frac{e^+(f) - e^-(f)}{e^+(f) + e^-(f)} \qquad \sigma_R(f) = \frac{e^v(f) - e^b(f)}{e^v(f) + e^b(f)}$$

$z^{\pm} = v \pm b$ Elsasser variables

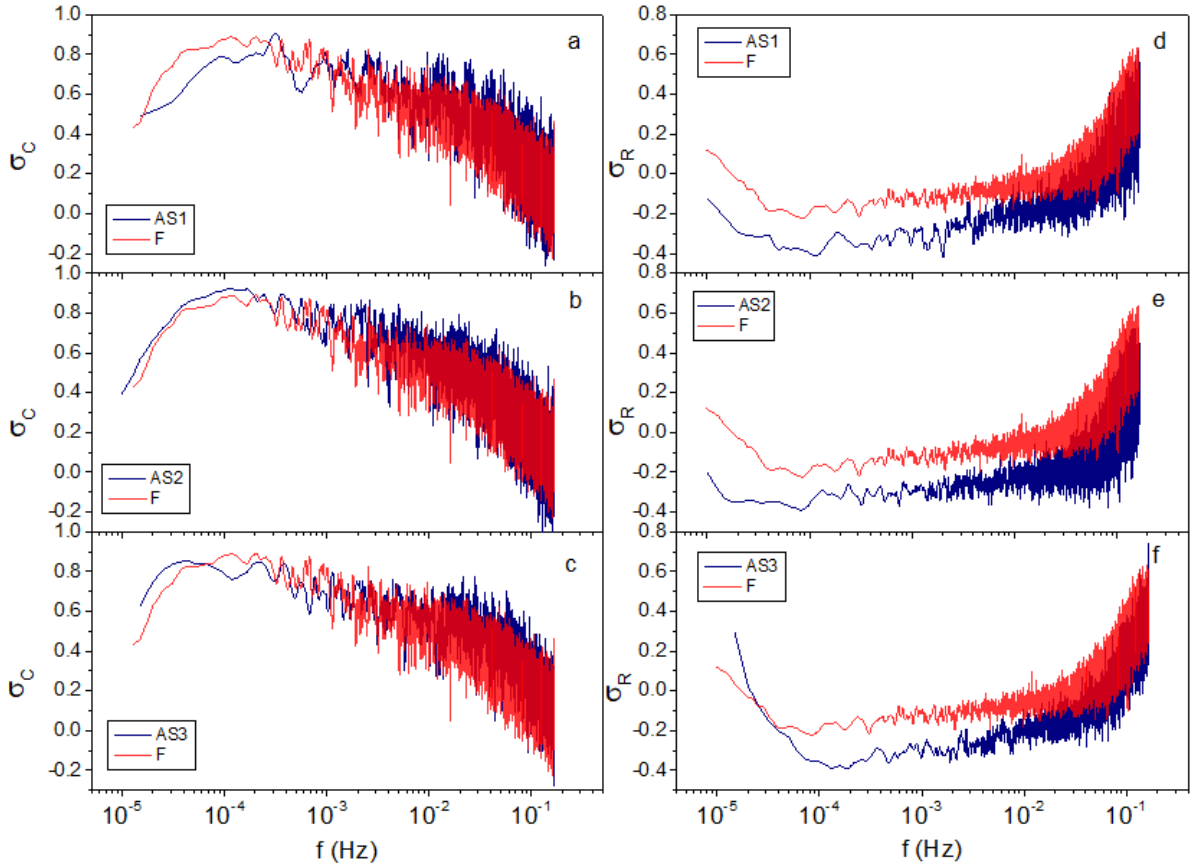

(D'Amicis et al., Universe, 2022)

Comparison between fast (F, red) and Alfvénic slow streams (AS1, AS2, AS3, blue)

σ_C : similar spectral behaviour for fast wind and Alfvénic slow streams

σ_R: fast wind is generally closer to equiparition

Alfvénic slow wind in the inner heliosphere

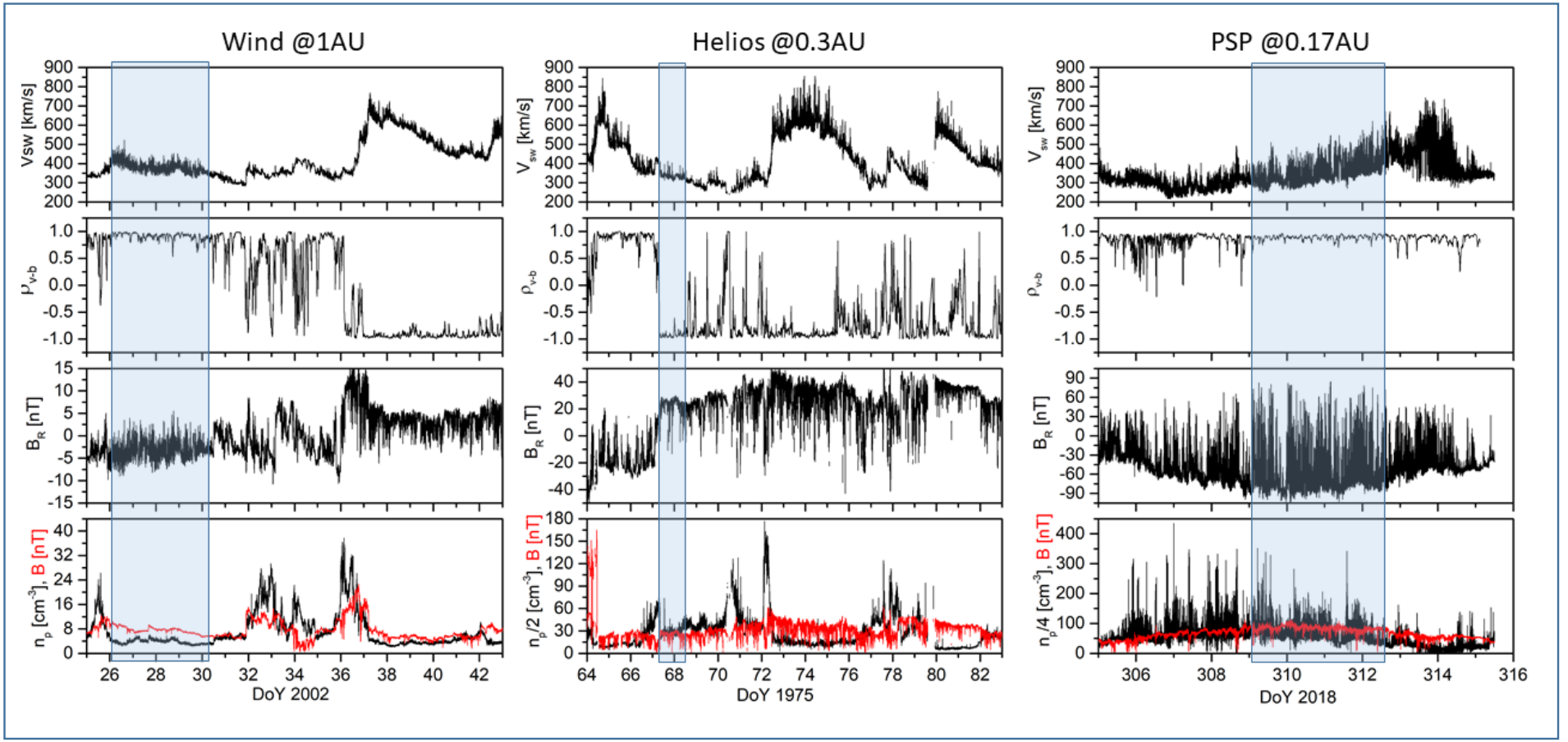

(D'Amicis et al, JGR, 2021)

PSP observations have shown the occurrence of the Alfvénic slow wind at all perihelion passages.

Spectral properties

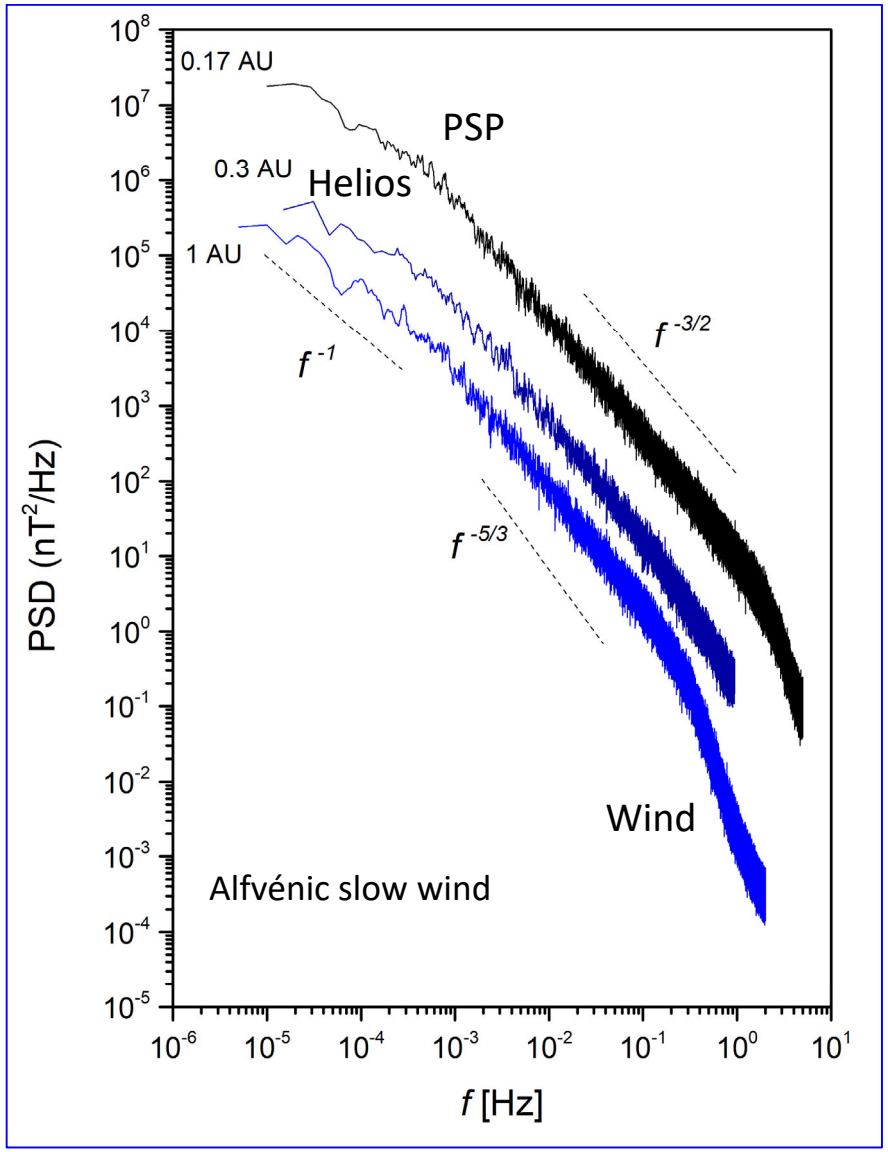

(D'Amicis et al, JGR, 2021)

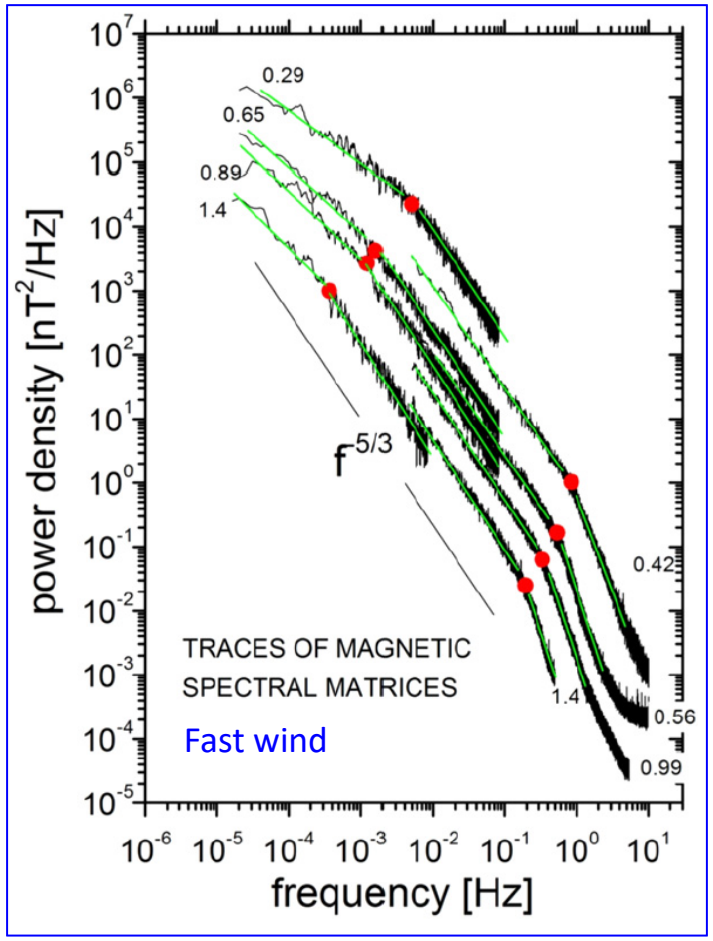

(Telloni et al, ApJ 2015)

Radial evolution of the spectral breaks in the fast wind

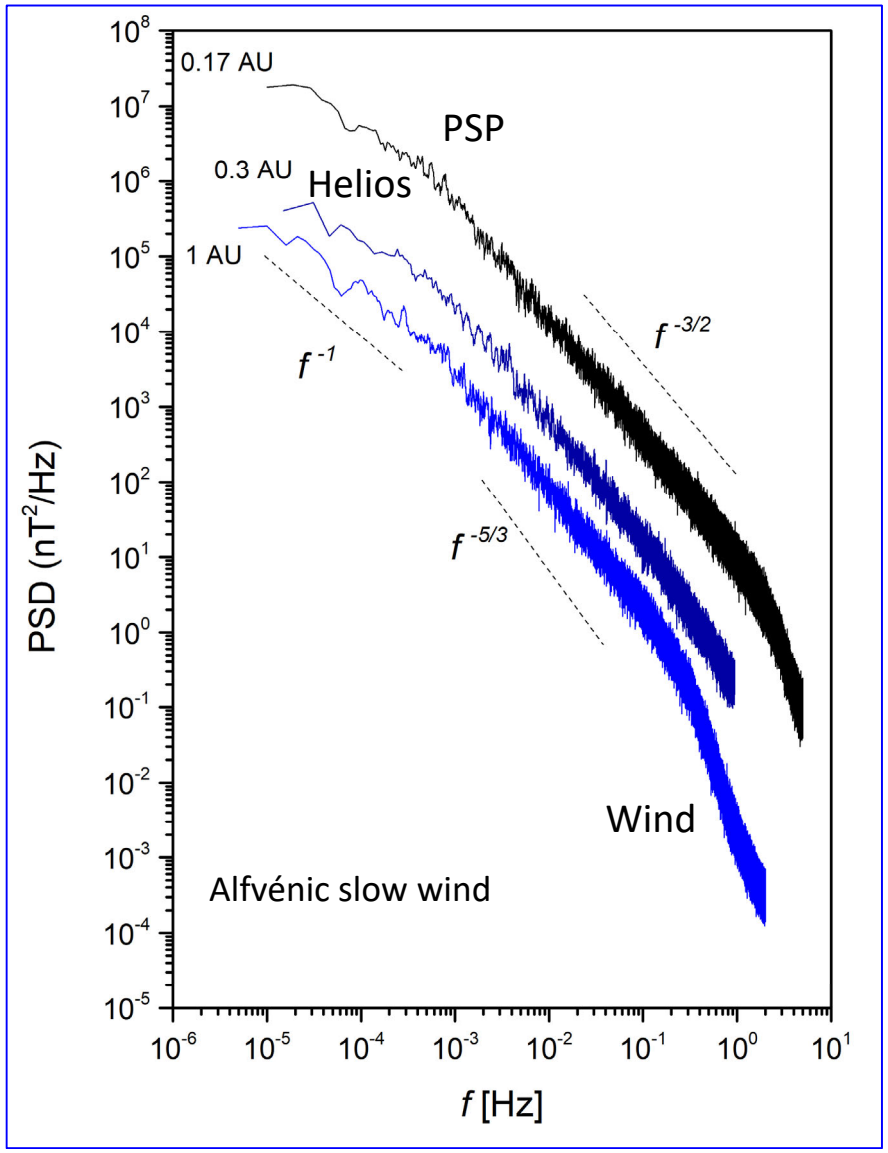

(D'Amicis et al, JGR, 2021)

Spectral properties

Three frequency ranges:

- 1/f regime; low-frequency break moving to lower frequencies as the wind expands probably linked to the saturation of magnetic field fluctuations (Matteini et al 2018 for fast wind and Bruno et al 2019, D'Amicis et al 2020, Perrone et al 2020 for slow wind).
- At intermediate scales, the radial evolution suggests a transition from a Kraichnan-like scaling of the power density toward a Kolmogorov-like scaling as the heliocentric distance increases (in agreement with Chen et al 2020).
- At the end of the inertial range, a spectral break, interpreted as a transition to kinetic turbulence, is observed. This break moves to lower frequencies as the solar wind travels in the inner heliosphere (in agreement with Duan et al 2020).
- Strong dependence of the observed spectral slope at ion scales on the power characterizing the fluctuations within the inertial range (see also Bruno et al 2014, D'Amicis et al 2019).

1/f scaling

(See also Matthaeus & Goldstein1986; Dmitruk & Matthaeus 2007; Verdini et al. 2012)

The 1/f scaling may be linked to the **saturation of the magnetic field fluctuations** in both fast (Matteini et al 2018) and slow (Bruno et al 2019, D'Amicis et al 2020, Perrone et al 2020) wind. However, for the non-Alfvénic slow wind, the 1/f scaling is recovered only if the interval is long enough (Bruno et al 2019) and provided that directional fluctuations are much larger than the compressive ones.

PDF of δ**B**/**B** at different scales

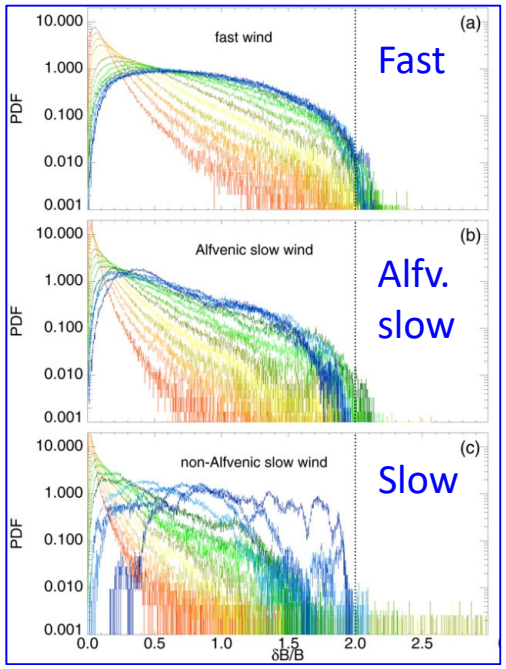

$\delta\mathbf{B} = \mathbf{B}(t+\Delta t) - \mathbf{B}(t)$

The maximum amplitude δ**B** is twice the radius of the sphere, i.e., δB≤2B.

Constant B magnitude

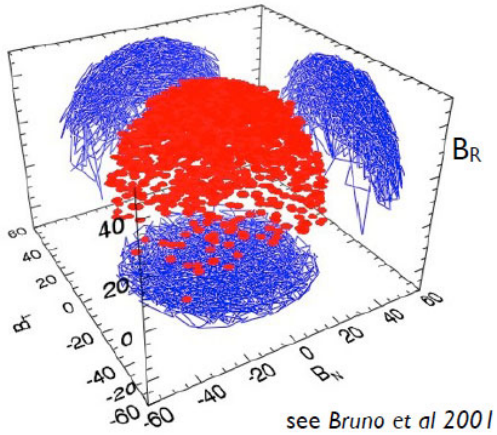

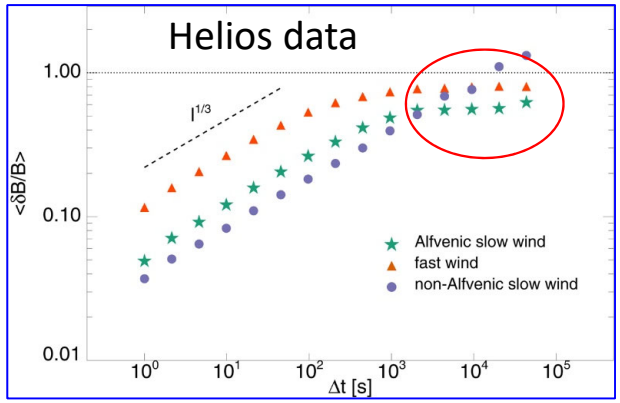

The low-frequency break of the spectrum corresponds to the scale at which the magnetic fluctuations saturate, limited by the magnitude of the local magnetic field, ⟨δB/B⟩ ≤1

(Perrone et al, A&A, 2020)

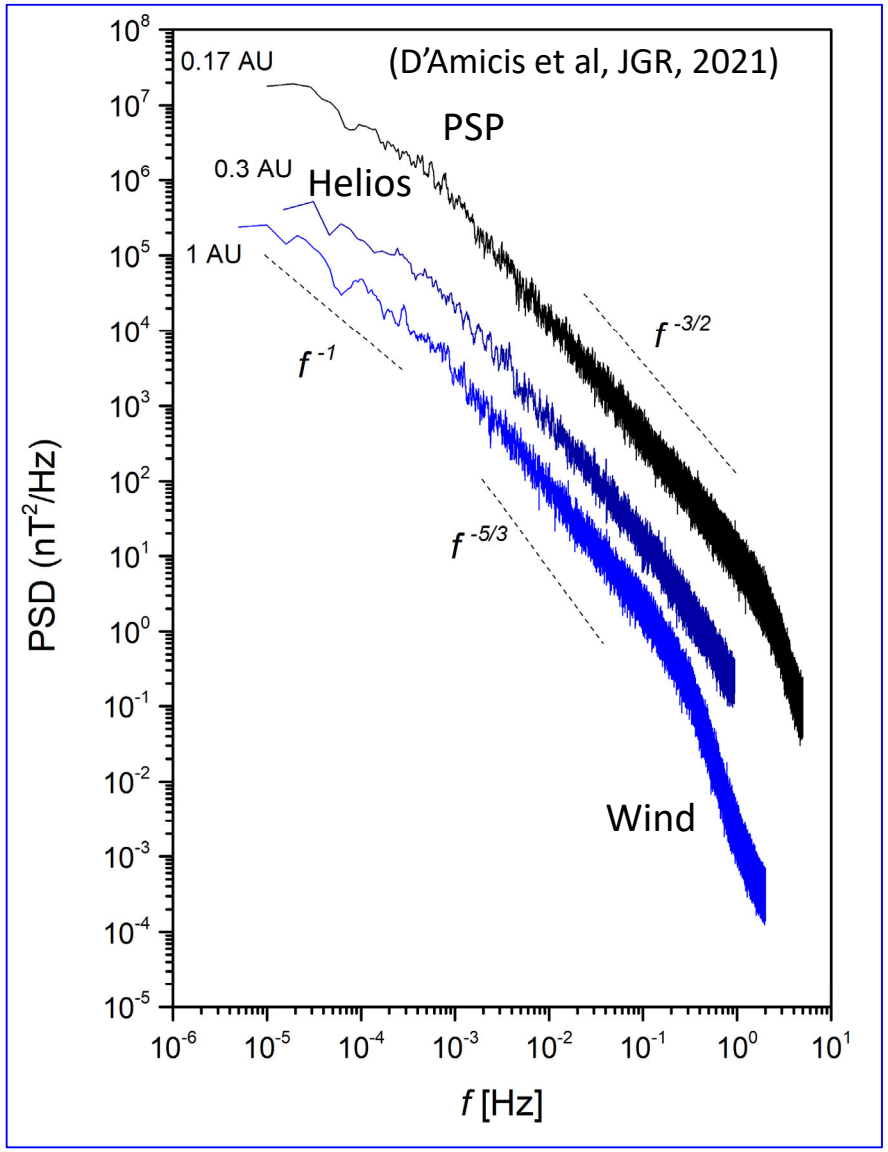

Spectral properties

Alfvénic slow wind - PSP

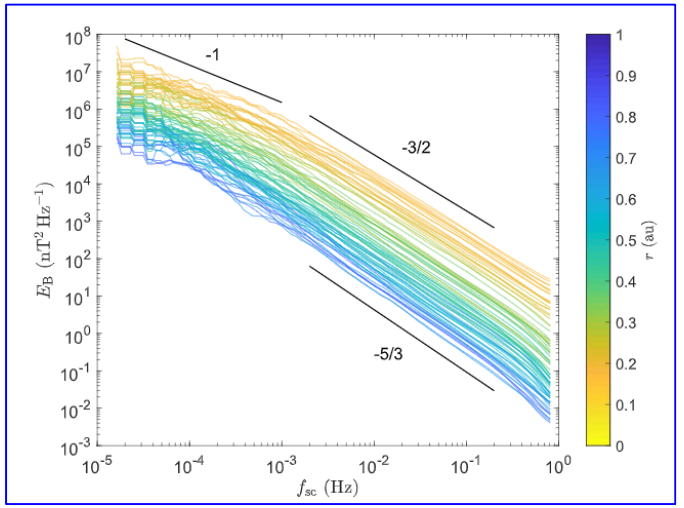

(Chen et al, ApJS, 2020)

A clear transition in the inertial range can be seen from α= −3/2 (Iroshnikov-Kraichnan) at r≈0.17 AU to α≈−5/3 (Kolmogorov) at r≈0.6 AU.

Spectral Break at Kinetic scales

PSP @ 0.17-0.62 AU

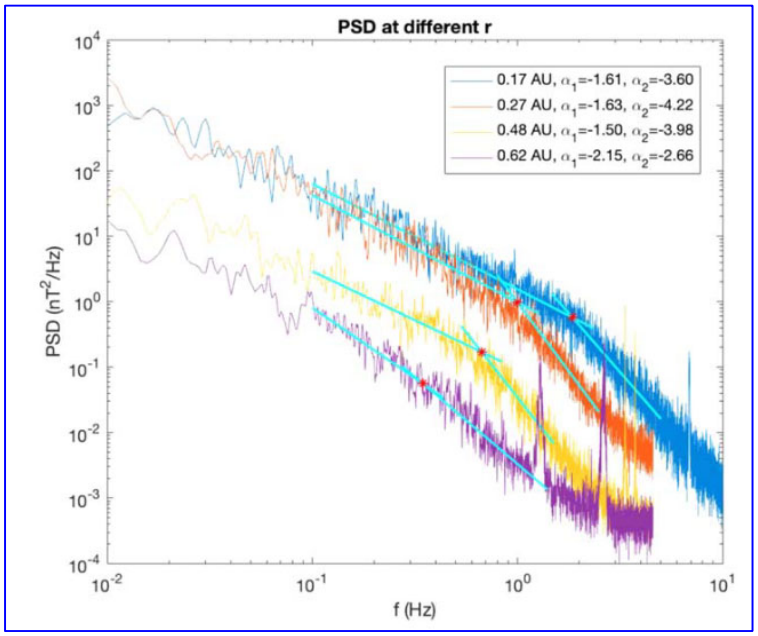

(Duan et al, ApJS, 2020)

The kinetic break in the Alfvénic slow solar wind has a radial dependence similar to the fast wind.

Bruno & Trenchi (2014) first found that the location of the kinetic break matches the wavenumber corresponding to the resonance condition for parallel-propagating Alfvén waves rather than the ion inertial length and the Larmor radius (Telloni et al 2015; Wang et al. 2018; Woodham et al. 2018; D'Amicis et al, 2019).

Linking fluid and kinetic scales

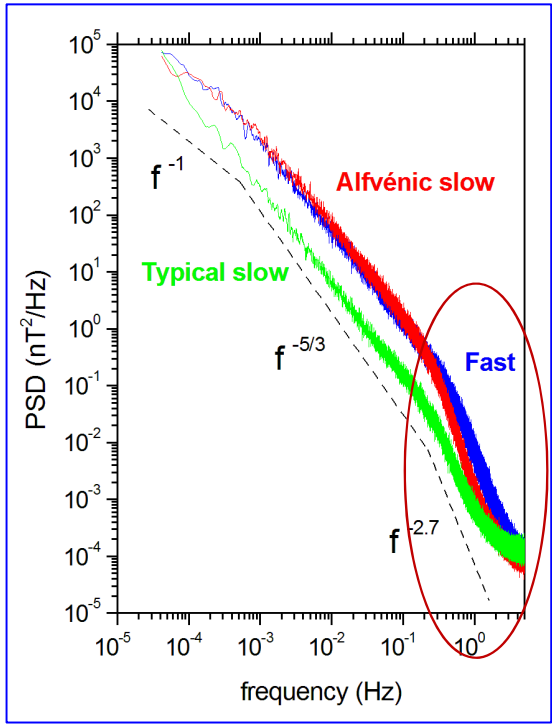

The steepening of the spectral index possibly implies that cascaded energy at the end of MHD scale may be gradually dissipated.

Strong dependence of the observed spectral slope at ion scales on the power characterizing the fluctuations within the inertial range: the higher the power, the steeper the slope in agreement with Bruno et al (2014).

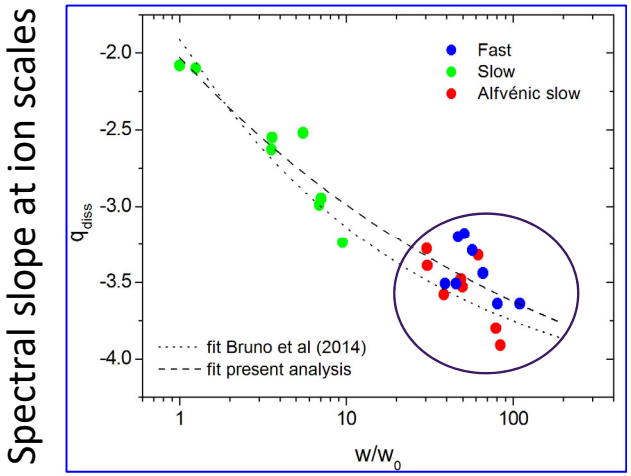

Power in the inertial range

Fast and Alfvénic slow streams

(D'Amicis et al, MNRAS, 2019)

Solar Orbiter observations

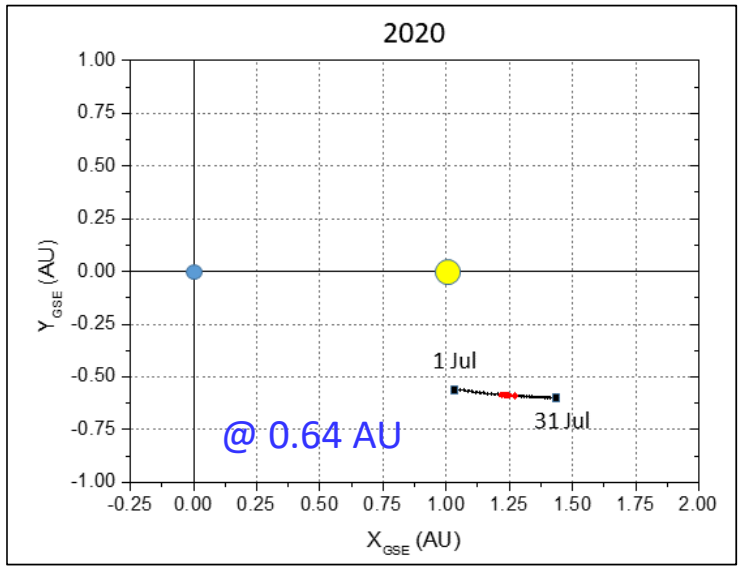

- Plasma moments: Solar Wind Analyzer (SWA)
- Magnetic field: Magnetometer (MAG)
- 4 s resolution

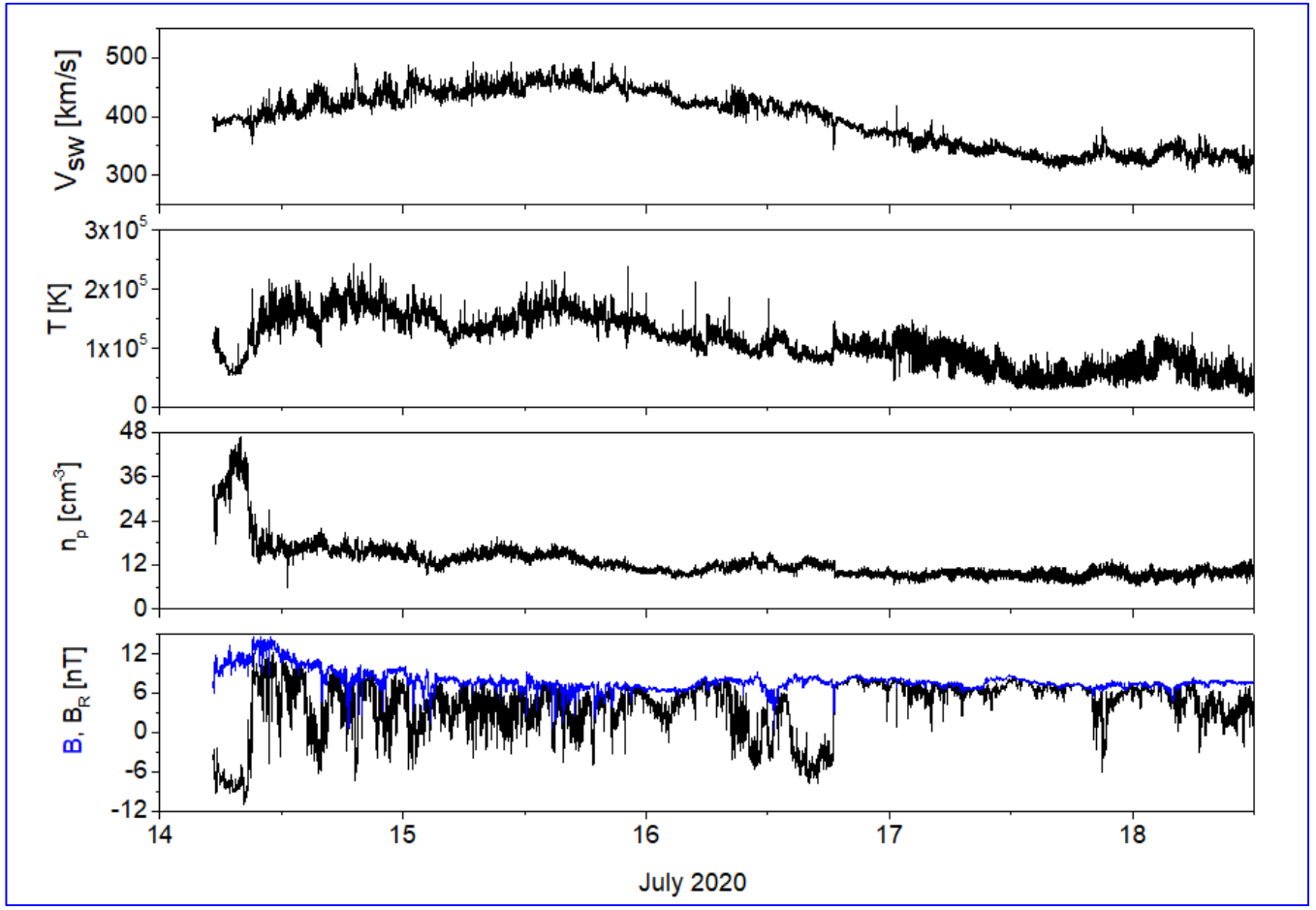

(D'Amicis et al, A&A, 2021, Solar Orbiter special issue)

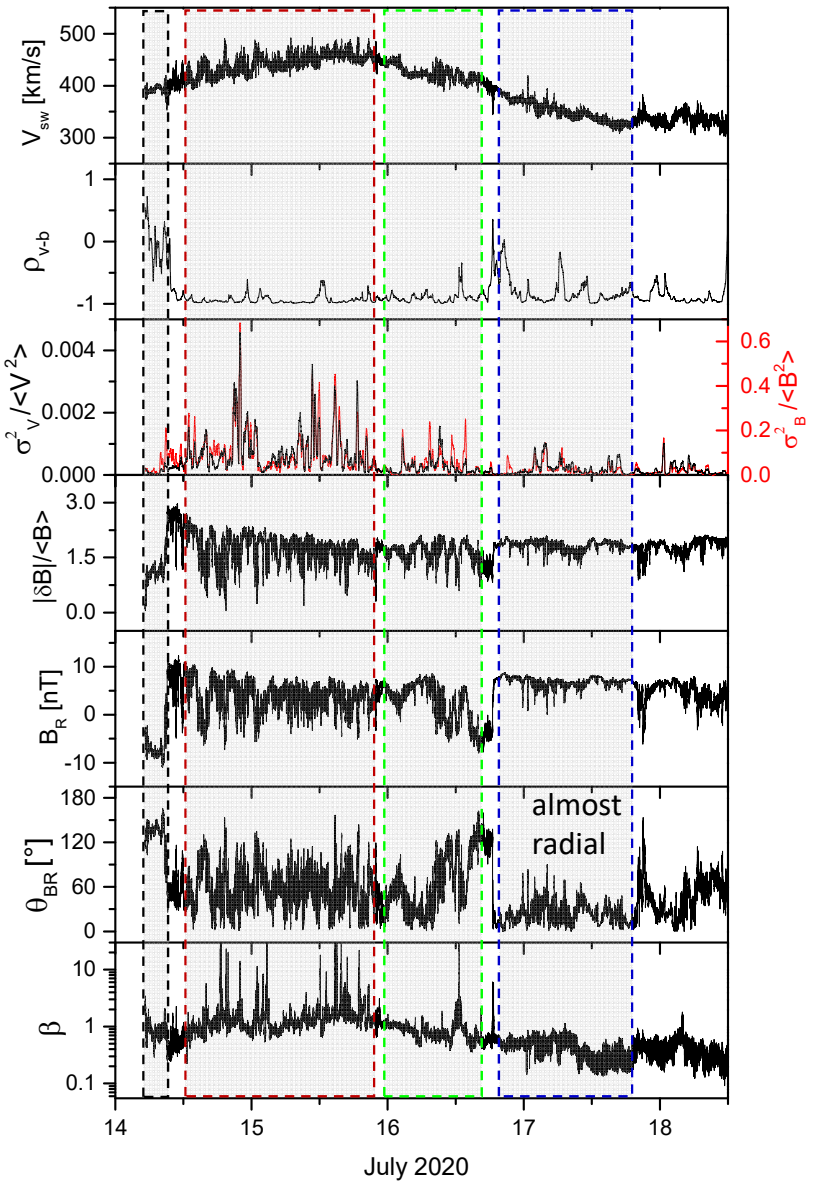

Alfvénic solar wind stream

Different regions: compression region, a main portion of the stream and a rarefaction region similar to a fast wind stream

v-b correlation coefficient: Alfvénic interval

Amplitude of the fluctuations: larger in the main portion

Vector displacement $|\delta\mathbf{B}(t)|/\langle B\rangle = \sqrt{\sum_i (B_i(t) - B_i(t_0))^2}/\langle B\rangle$

Presence of switchbacks

Different orientation of B respect to the radial

Different behavior of plasma β

(D'Amicis et al, A&A, 2021)

Spectral properties

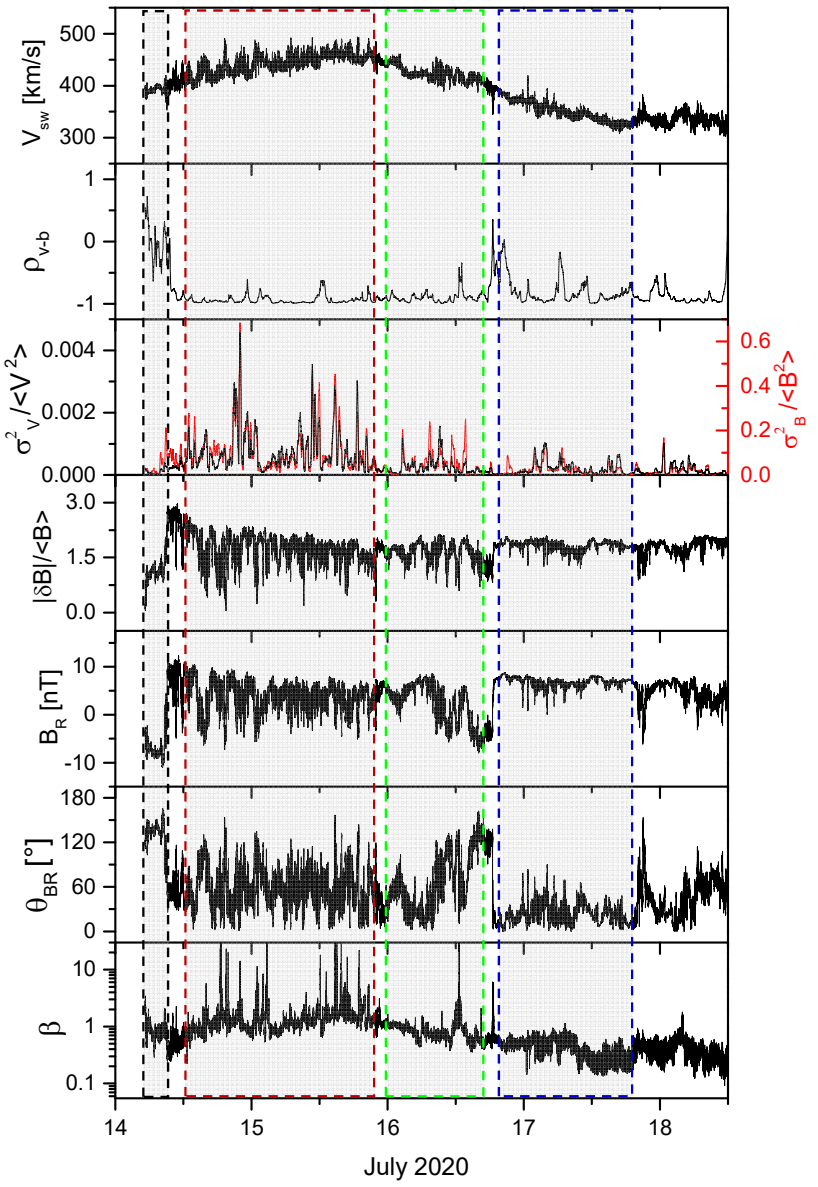

Three frequency ranges:

- 1/f
- Inertial range
- Kinetic range

Higher power of the fluctuations in the main portion of the stream in agreement with the present of large amplitude Alfvénic fluctuations.

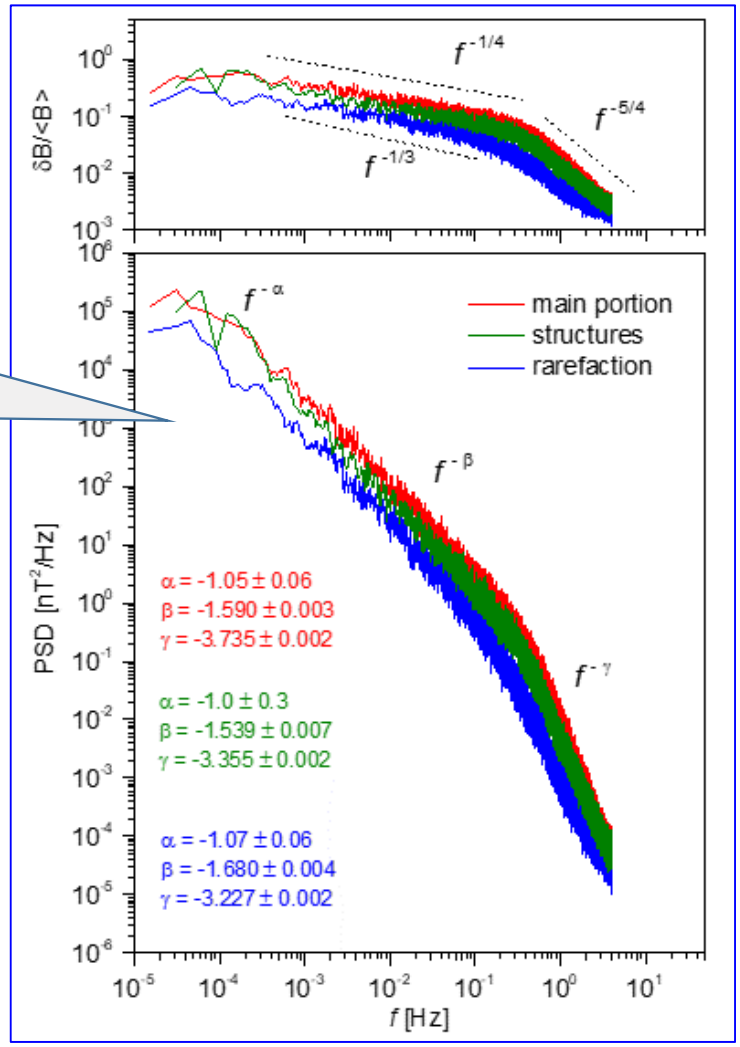

(D'Amicis et al, A&A, 2021)

Nature of magnetic fluctuations

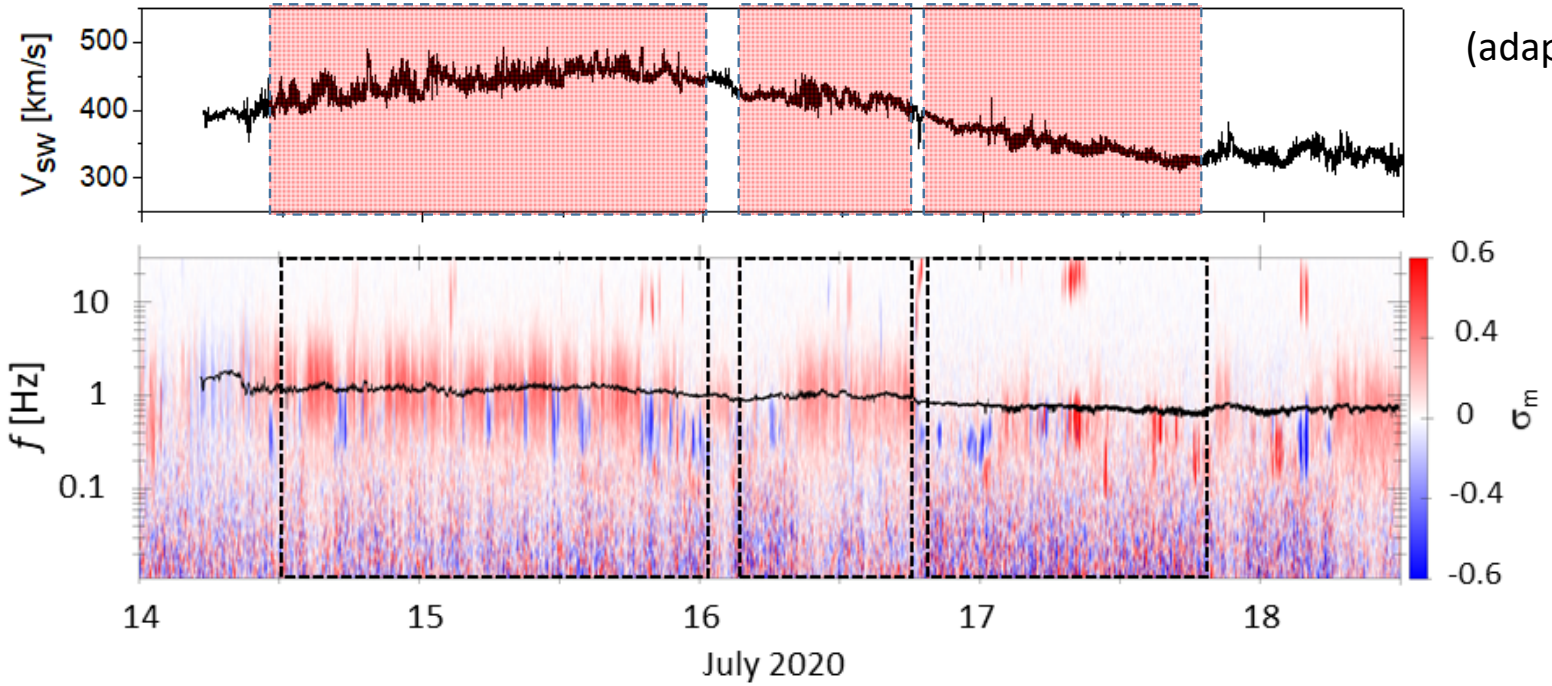

(adapted from D'Amicis et al, A&A, 2021)

$$\sigma_m(t,f) = \frac{2\Im\left\{\mathcal{W}_T^*(t,f)\,\mathcal{W}_N(t,f)\right\}}{|\mathcal{W}_R(t,f)|^2 + |\mathcal{W}_T(t,f)|^2 + |\mathcal{W}_N(t,f)|^2}$$

Normalized magnetic helicity

Different regions and different magnetic helicity signatures

Coherent magnetic helicity signatures are predominant in the main portion of the stream, rather than in the intermediate region. Their occurrence rate in the rarefaction region is even lower.

Magnetic helicity signatures at proton scales consistent with previous studies (He et al. 2011, 2012a,b; Podesta & Gary 2011; Klein et al. 2014; Bruno & Telloni 2015; Telloni et al. 2015; Telloni & Bruno 2016; Telloni et al. 2019, 2020; Woodham et al. 2019, 2021)

Waves in the Alfvénic slow wind

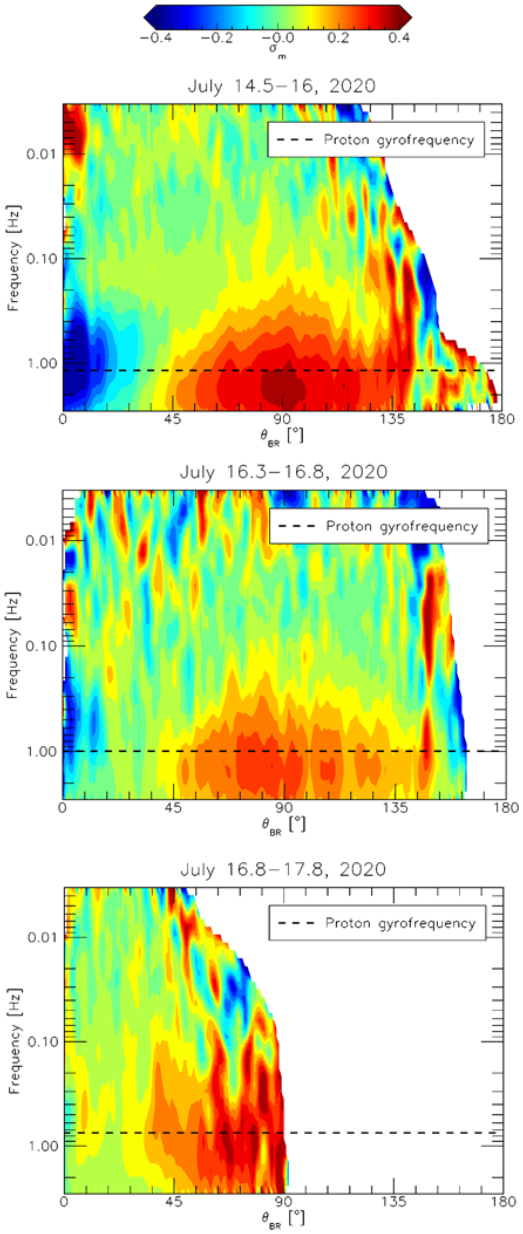

Main portion

$$\sigma_m(t,f) = \frac{2\Im\left\{\mathcal{W}_T^*(t,f)\,\mathcal{W}_N(t,f)\right\}}{|\mathcal{W}_R(t,f)|^2 + |\mathcal{W}_T(t,f)|^2 + |\mathcal{W}_N(t,f)|^2}$$

Normalized magnetic helicity

Structures

For an outward propagating magnetic field, $\sigma_m(\theta_{VB},f)$ shows the signatures of quasi-parallel left-handed polarization **ICWs** ($\sigma_m<0$ at $\theta_{VB}>45°$) and quasi-perpendicular right-handed polarization **KAWs** ($\sigma_m>0$ at $45°<\theta_{VB}<130°$), as far as Alfvénicity and the amplitude of the fluctuations are relevant.

Rarefaction region

Results in agreement with a previous study at 1 AU on the Alfvénic slow wind (Telloni et al 2020) and on the fast wind (Bruno & Telloni 2015, Telloni & Bruno, 2016).

(D'Amicis et al, A&A, 2021)

Solar Orbiter magnetic connectivity

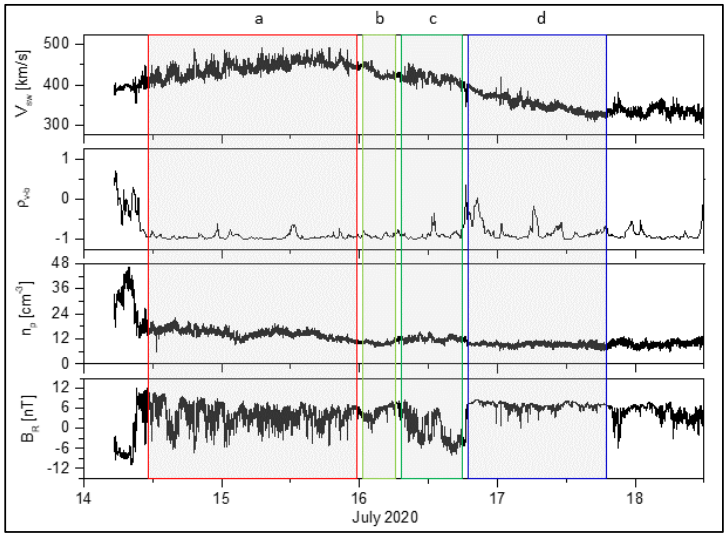

Gradual changes in the magnetic connectivity –

a) from the internal part of the northern positive polar coronal hole extension,
b) to its eastern boundary,
c) to a short connection with the negative open field area at the equator,
d) to the double coronal hole connections separated by a pseudostreamer.

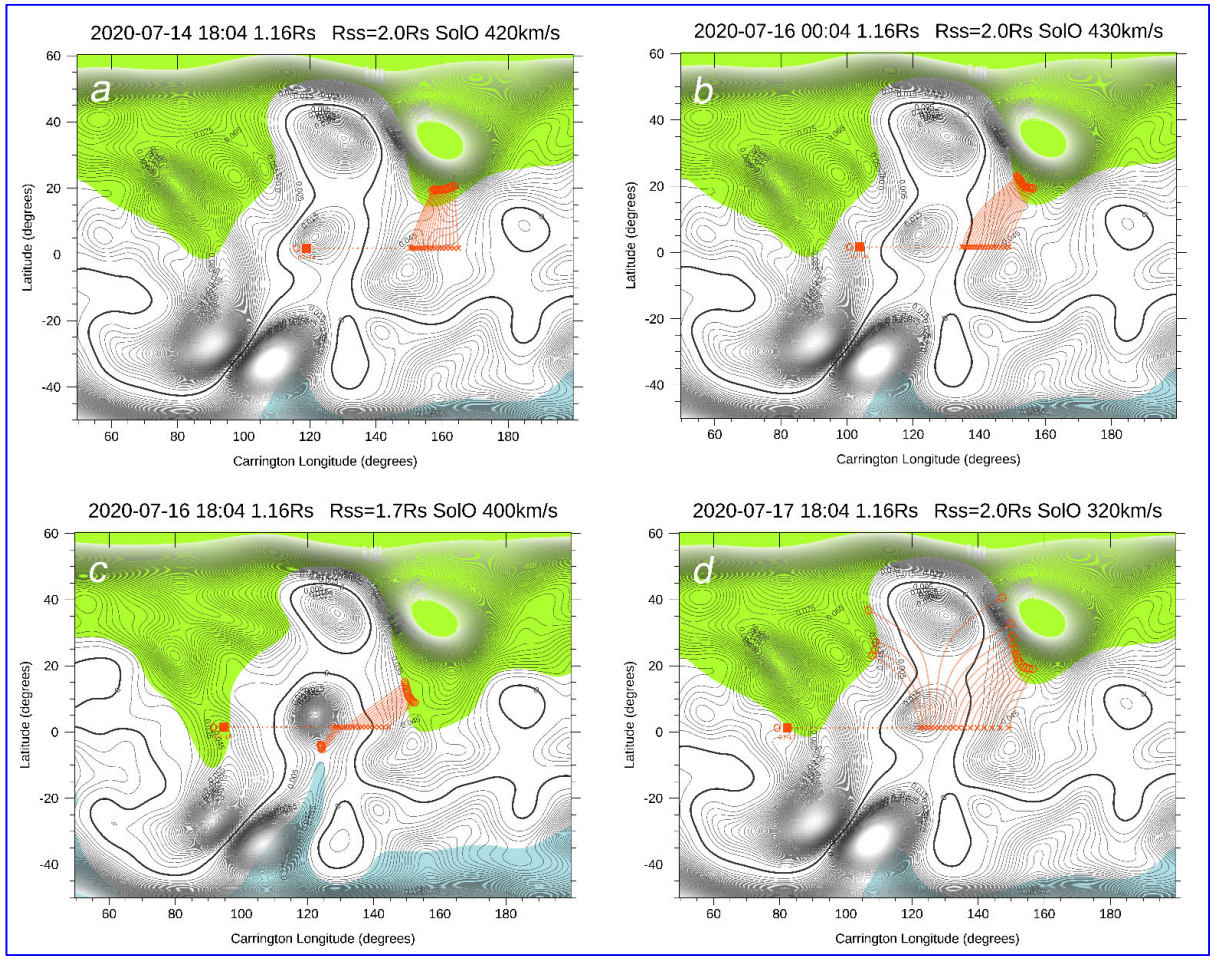

(D'Amicis et al, A&A, 2021)

Separating VDFs with Clustering and Gaussian Mixture Model

Total VDF

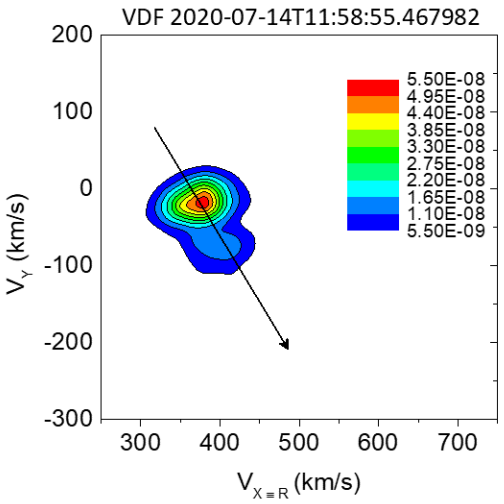

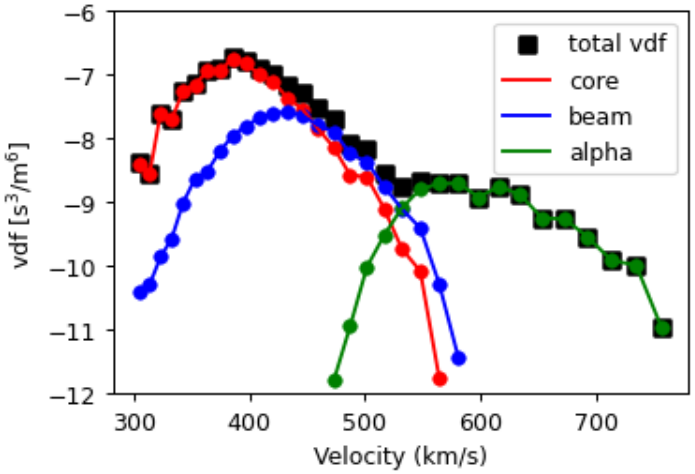

(De Marco et al, A&A, accepted)

Total VDF = **core** + **beam** + **alpha**

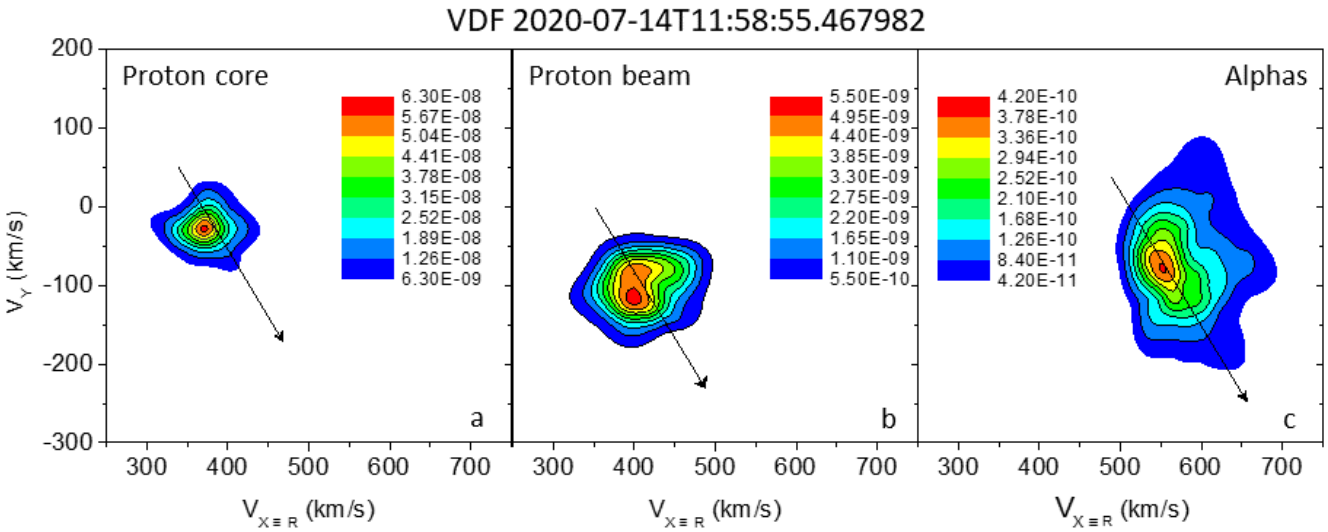

Derivation of moments (number density, velocity vector, temperature) of VDFs for the 3 populations

Innovative Code Based on Machine Learning to Separate Ion Families in 3D VDFs

In solar wind spectra, the moments of alpha particles and protons core and beams are usually computed applying bi-Maxwellian fit to each family. We introduced the **clustering** technique using the Gaussian Mixture Model (GMM).

In a GMM, measurements are distributed as a weighted mixture of normal distributions

$$p(\boldsymbol{x}) = \sum_{k=1}^{K} \pi_k \mathcal{N}(\boldsymbol{x} | \boldsymbol{\mu}_k, \boldsymbol{\Sigma}_k)$$

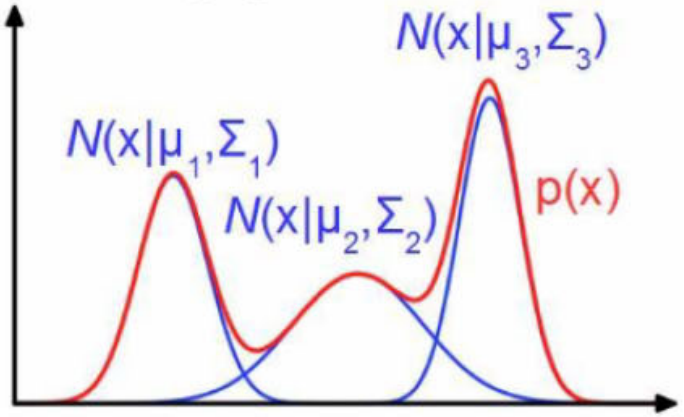

In clustering, the algorithm iteratively assigns to each data point a probability of belonging to one distribution which is a component of a mixture of several components.

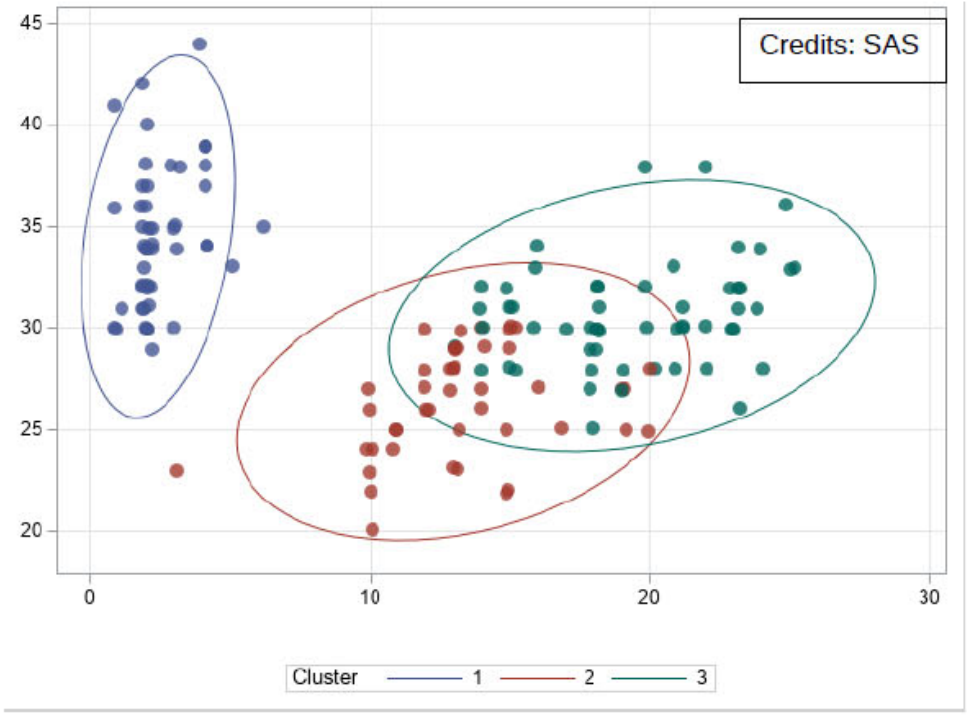

The parameters of the distributions and the membership of data is deduced solely from the arrangements of the points in the input space.

Investigating kinetic festures in Solar Orbiter observations of an Alfvénic slow stream

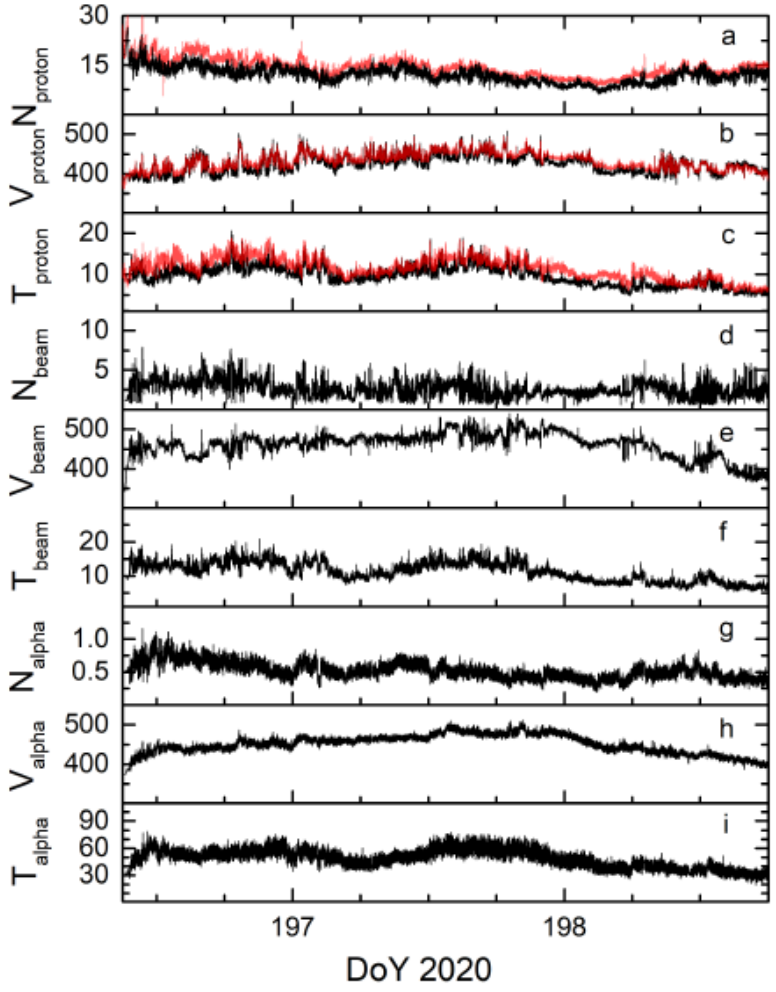

(De Marco et al, A&A, accepted)

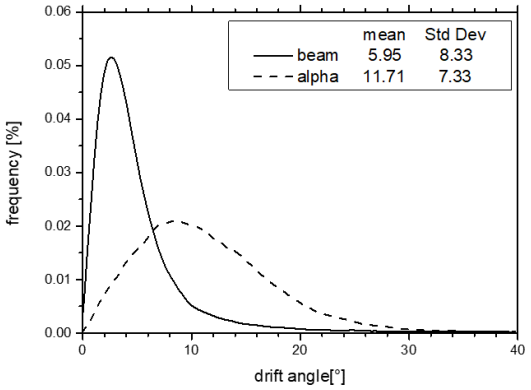

Results consistent with solar wind streams observed by Helios at the same radial distance.

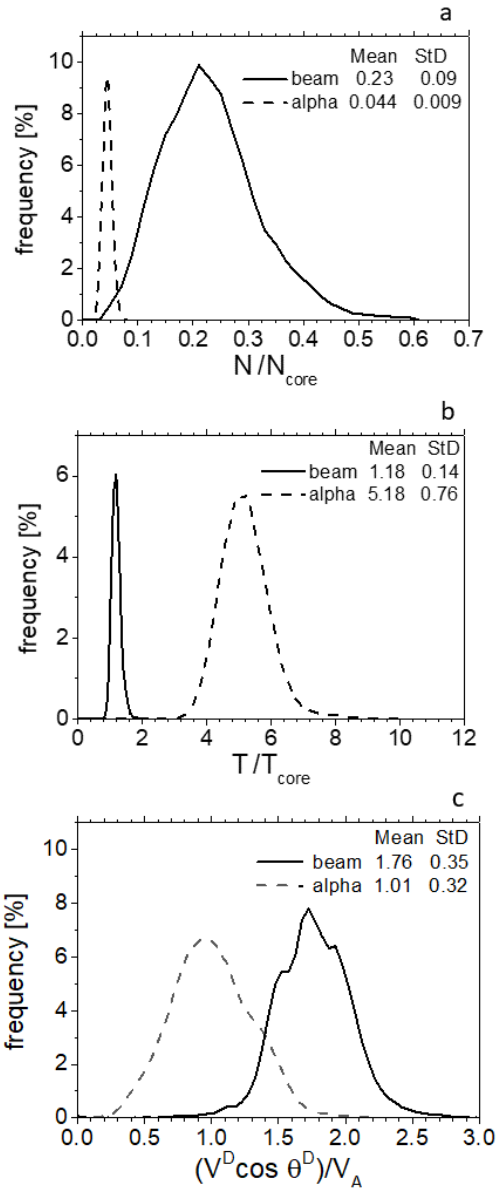

Proton core, proton beam and alpha in the instability plane

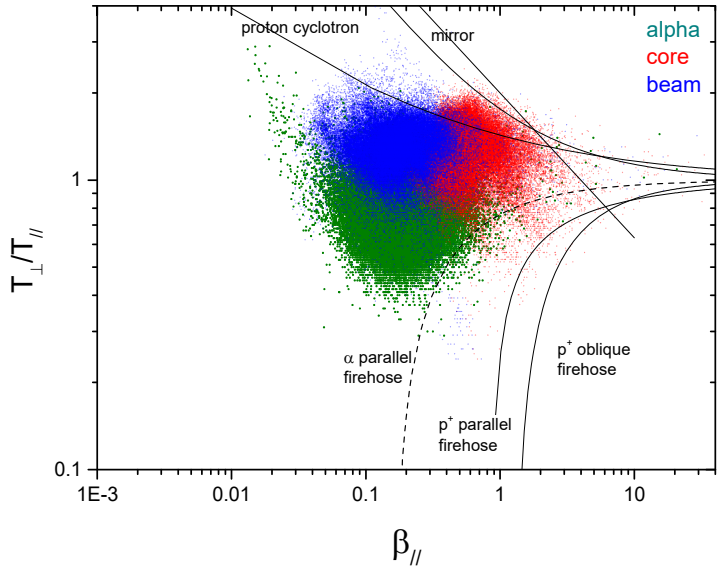

- the core population is regulated by the mirror instability while
- the beam population is constrained by the ion cyclotron instability
- the alpha population is regulated by the alpha parallel firehose

→ Currently performing a study on the radial evolution of kinetic features

Empirical relation by Tu et al 2004

$$v_d/v_A = (2.16 \pm 0.03)\,\beta_{\|c}^{(0.281\pm0.008)}$$

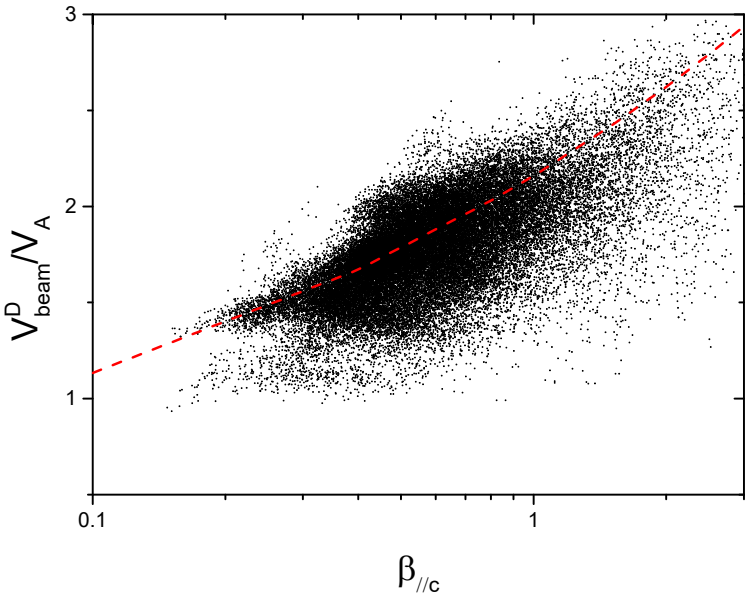

Constrain to solar wind models

Multi-point studies – different approaches:

- Study the solar wind at different heliocentric distances (not linked to each other)

  → Statistical approach

- Study the evolution of the same plasma parcel at different heliocentric distances (conjuctions)

  → Evolution of the solar wind

- Study the solar wind at different heliocentric distances coming from the same solar source

  → Evolution of the solar source

Telloni et al, ApJL, 912, L21, 2021

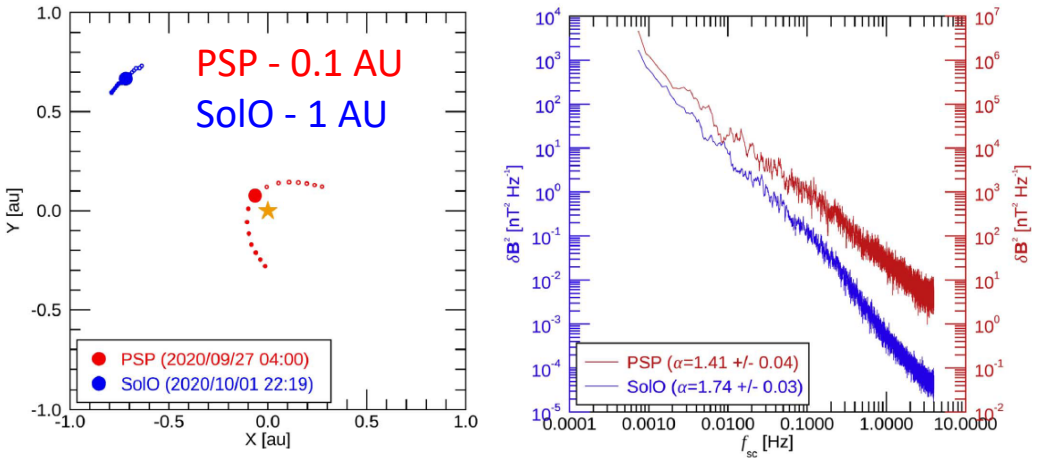

Alberti et al, ApJ, 926, 174, 2022

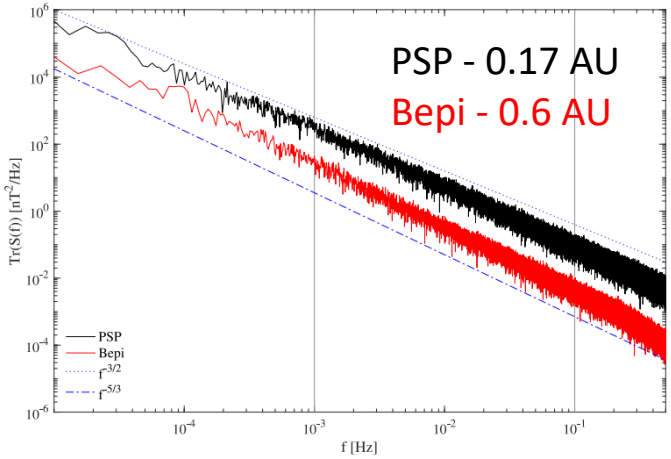

Studying conjuctions: PSP - SolO and PSP - Wind in 2021

Evolution of Alfvénicity in slow wind intervals observed at different distances (PSP at 0.1 AU, Solar Orbiter at 0.89 and Wind at 1 AU) and coming from the same solar source (D'Amicis et al, in preparation)

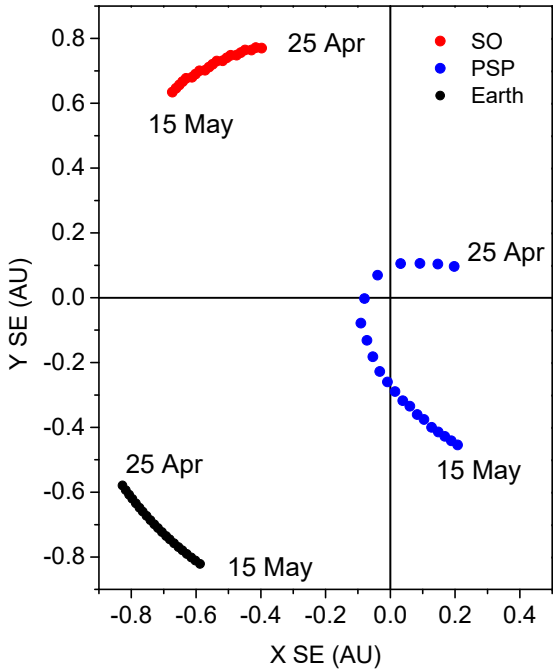

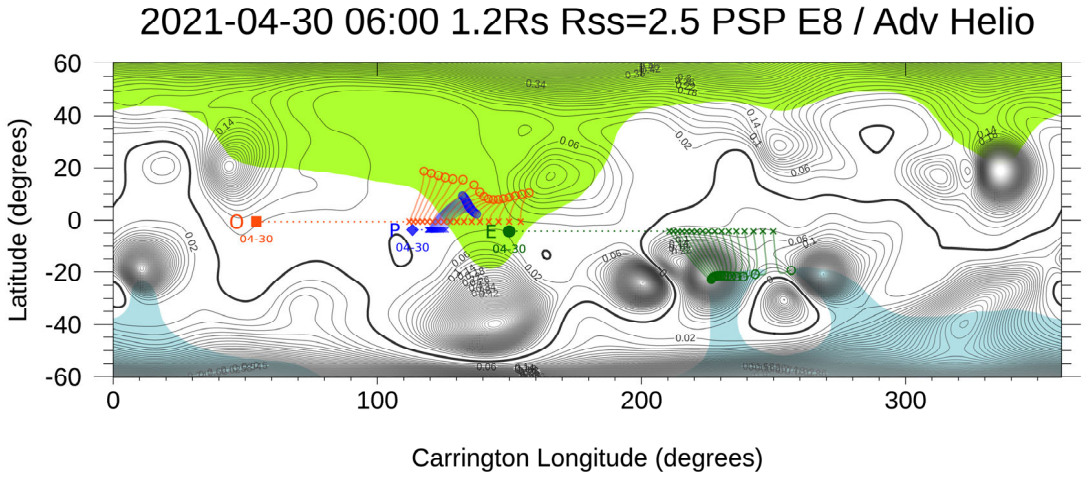

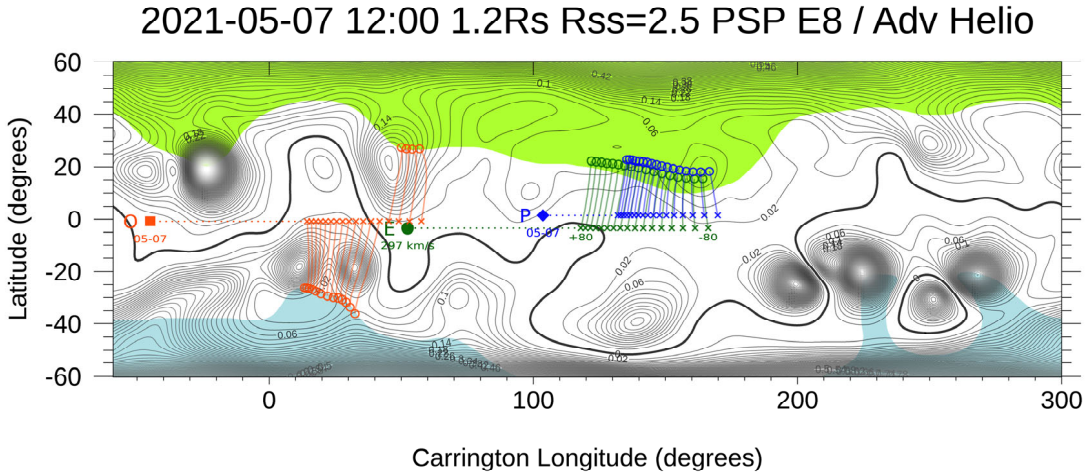

Studying conjuctions: PSP - SolO and PSP - Wind in 2021

Evolution of Alfvénicity in slow wind intervals observed at different distances (PSP at 0.1 AU, Solar Orbiter at 0.89 and Wind at 1 AU) and coming from the same solar source (D'Amicis et al, in preparation)

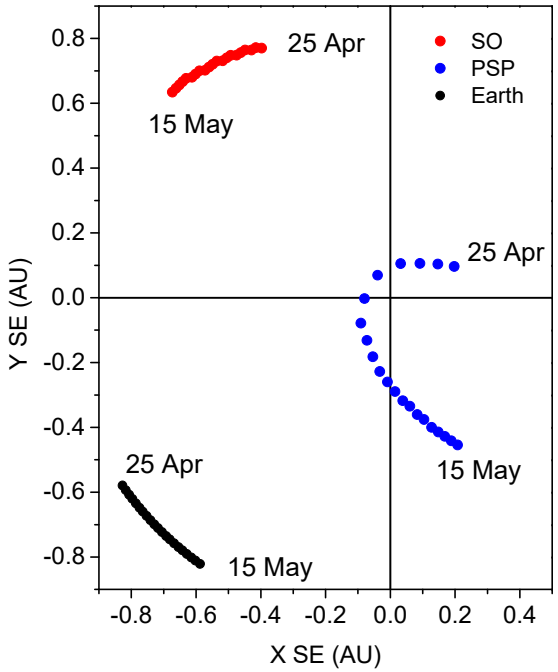

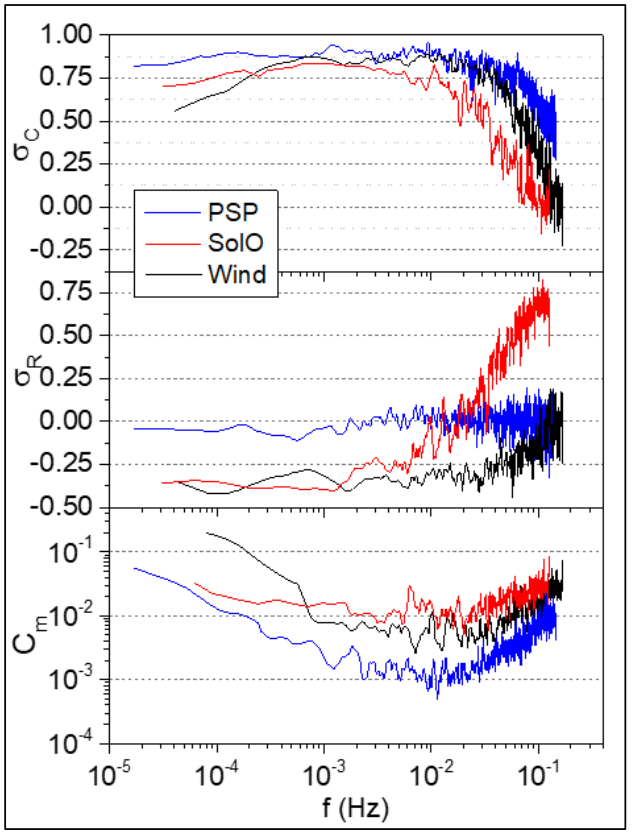

Evolution of Alfvénicity: increase of magnetic imbalance of solar wind fluctuations and of magnetic compressibility

Relevance

- Several similarities between fast and Alfvénic slow wind have been recovered at different radial distances and during different phases of the solar cycle.
- Similar solar source: regions of anomalous (greater than average) areal expansion of magnetic flux tubes near the Sun such as low-latitude small coronal holes and/or the boundaries of the polar coronal holes. Such regions may form easily when large-scale pseudostreamers are present in the corona.
- If both fast and Alfvénic slow wind originate from open field regions, then something must account for the difference in speed. The investigation of the Alfvénic slow wind is thus critical for the understanding of the solar wind acceleration in general.

Motivation

- PSP observations have shown the occurrence of the Alfvénic slow wind at all perihelion passages.
- Solar Orbiter and PSP are approaching the solar maximum during which a high occurrence of the Alfvénic slow wind is expected.

Future studies

Investigation of the differences between non-Alfvénic and Alfvénic slow wind and their evolution in the inner heliophere using mainly data from Solar Orbiter; studies of the kinetic features separating the main ion populations (core, beam and alpha) using a ML code